Study, Design and Analysis of Antennas for Millimeter Waves and UWB Applications

LAKHAN

A Thesis Submitted to
Indian Institute of Technology Hyderabad
In Partial Fulfillment of the Requirements for
The Degree of Master of Technology

भारतीय प्रौद्योगिकी संस्थान हैदराबाद
Indian Institute of Technology Hyderabad

Department of Electrical Engineering

June 2016

Declaration

I declare that this written submission represents my ideas in my own words, and where ideas or words of others have been included, I have adequately cited and referenced the original sources. I also declare that I have adhered to all principles of academic honesty and integrity and have not misrepresented or fabricated or falsified any idea/data/fact/source in my submission. I understand that any violation of the above will be a cause for disciplinary action by the Institute and can also evoke penal action from the sources that have thus not been properly cited, or from whom proper permission has not been taken when needed.

(Signature)

Lakhan

(LAKHAN)

EE13M1025

(Roll No.)

Approval Sheet

This Thesis entitled Study, Design and Analysis of Antennas for Millimeter Waves and UWB Applications by LAKHAN is approved for the degree of Master of Technology from IIT Hyderabad.
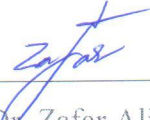
Dr. Sumohana Channappayya

Examiner

Dr. Abhinav Kumar

Examiner

Dr. Siva Rama Krishna Vanjari

Adviser

Dr. Zafar Ali Khan

Co-Adviser

Dr. Pankoj S. Kolhe

Chairman

Acknowledgements

The present study and thesis would not be complete without acknowledging the support and encouragement from the people mentioned here.

Firstly, I would express my gratitude towards my project advisor Dr. Siva Vanjari and Dr. Zafar Ali Khan, who motivated me to work harder and their constant help and guidance encouraged me to work more interestingly in this field.

I would like to thank my colleague and friend Shrutika who was always there to help and support me to complete this work.

I would like to thank my friend Murali Krishna for helping me to improve my writing capability by giving feedbacks. I would like to thank all my professors from the department whose lectures have helped me to broaden my vision and also the confidence I gained because of the term projects given by them which were to be completed in a small span of time.

I would like to thank my parents for their support of all aspects of my life, but especially of my education.

Dedication

To Family and Friends

Abstract

Since the release by the Federal Communications Commission (FCC) of a license free UWB (Ultra Wide Band) bands mainly offering bandwidth of 7.5 GHz (from 3.1 GHz to 10.6 GHz) and UWB at Millimeter(MM) wave frequency centred at 60 GHz (57 GHz to 64 GHz) for wireless communications, UWB is rapidly advancing as a high data rate wireless communication technology.

As is the case in conventional wireless communication systems, antennas plays a very crucial role in UWB systems. However, there are more challenges in designing a UWB antenna than designing narrow band one. A suitable UWB antenna should be capable of operating over an UWB as allocated by the FCC. At the same time, satisfactory radiation properties over the entire frequency range with minimal distortion are also necessary.

This thesis focuses on UWB antenna design and analysis for two different frequency bands, the first UWB antenna designed for frequency range from 3.1 GHz to 10.6 GHz and the second one is a MM wave UWB antenna which is centred around 60 GHz and ranges from 57 GHz to 64 GHz. Studies have been undertaken covering the areas of UWB fundamentals and antenna theory. Extensive investigations and theoretical analysis were also carried out on proposed UWB antennas.

In this work literature survey is carried out about different antenna structures used for UWB applications. To design antenna for UWB (3.1 GHz to 10.6 GHz), studies have been carried out and four Swastika-shaped slot antenna designs have been proposed. Both ground plane and radiating patch are modified in proposed antennas. In first three antenna designs (antenna design 1, antenna design 2, antenna design 3) the radiating patch is modified with concentric circular slots of different dimensions while in antenna design 4, two inverted L-shaped slots on ground plane are used to achieve enhanced bandwidth and reduced return losses. All these proposed novel antennas are of compact size having dimensions of 24 mm x 24 mm and they almost cover entire UWB range (3.1 GHz to 10.6 GHz). The antenna parameters like bandwidth, return loss, radiation pattern and impedance of these antennas are analyzed and discussed in chapter 2.

Further two tetraskelion (swastika-shape) designs (Design 1 and Design 2) are optimized to improve the bandwidth by varying the shape and dimensions of the notches in Design 1 and Design 2. As a result, Design 1 operates in the frequency range of 3.65 GHz to 11.03 GHz and Design 2 operates in the frequency range of 3.68 GHz to 10.69 GHz.

MM wave UWB technology has been studied and design issues and the effect of MM waves have been explored by extensive literature survey. Interaction of MM waves with human body, its propagation in the atmosphere and difficulties related to it, are also studied. All parameters and physics involved behind analysis of antenna structure mathematically have been exploited by taking reference of linear dipole antenna.

An antenna of non-linear geometry which can be categorised as thin-wire dipole whose length is half of the wavelength, have been designed for UWB applications which can cover whole bandwidth (7 GHz) of unlicensed band centred at 60 GHz which ranges from 57 GHz to 64 GHz (FCC standards for US) for fast wireless communications. Radiation pattern and other antenna parameters for this non-linear antenna have been derived and the obtained theoretical results are plottted using MATLAB tool.

All simulations are done in High frequency Stucture Simulator (HFSS).

Contents

Chapter 1

Introduction

1.1 Introduction

UWB is emerging tremendously these years. Due to its large operating bandwidth it is best suited for applications like high data rate wireless communications, imaging systems, high accuracy radars, health-care and personal entertainment. UWB antenna technology is one of the advanced technologies in this modern world [1]. Federal Communications Commission (FCC) has approved 7.5 GHz bandwidth between 3.1 GHz and 10.6 GHz for the unlicensed UWB communications [2]. In recent years, UWB radars sensors are used in medicine [4] and short range vehicular applications [5]. Different types of UWB antennas have been proposed which include printed monopole antennas [6], [7], [8], single ended elliptical antennas [9]. MMwave generally corresponds to the radio spectrum between 30 GHz to 300 GHz, with wavelength between one to ten millimeters. However, in the context of wireless communication, the term generally corresponds to a few bands of spectrum near 38, 60 and 94 GHz, and more recently to a band between 70 GHz and 90 GHz (also referred to as E-Band), that have been allocated for the purpose of wireless communication in the public domain.

1.2 Objective of Work

This work mainly focused on designing antennas for UWB applications which can work in whole available bandwidth of following unlicensed frequency bands available (by FCC):
1. UWB : 3.1 GHz to 10.6 GHz
2. UWB : 57 GHz to 64 GHz
To design and analyse a compact antenna for unlicensed UWB centred at 60 GHz which can be easily embroidered on fabric to avoid costly fabrication processes as required in planar antennas. The main objective of the work is to analyze all the relevant parameters and prove the same with theoretical model using mathematical equations which should reasonably be concurrent with the obtained simulation results To design and optimize a planar monopole patch antenna for 3.1 GHz to 10.6 GHz UWB.

1.3 Contribution of This Thesis

- Antennas have been designed for two different UWB frequency ranges.

- A non-linear MM wave thin-wire half-wavelength dipole antenna is designed, and analysed for unlicensed UWB available at 60 GHz frequency (57 GHz to 64 GHz).

- Antenna parameters are derived theoretically for the non-linear structure and those derived results are plotted using MATLAB tool. These results are validated by comparing with simulated results obtained by simulating same non-linear structure using HFSS tool.

- Four Swastika slot antenna designs have been proposed and optimized for 3.1 GHz to 10.6 GHz unlicensed UWB.

1.4 Thesis Organization

- Chapter 1: is the introduction describing the objective behind the work and contributions of this thesis.

- Chapter 2: describes basics about monopole antennas and its different types, proposed four UWB swastika-shaped antenna designs and their comparison. Further two among these four designs are optimized which are also discussed.

- Chapter 3: describes the basics of linear dipole antenna its characteristics.

- Chapter 4: describes study of antennas at MM wave frequencies, its effects on human body and its application.

- Chapter 5: describes a compact non-linear MM wave antenna for UWB applications and all antenna parameters are derived.

- Chapter 6: concludes the thesis and discusses future work.

Chapter 2

UWB Antennas

2.1 Why UWB Antenna?

In order to achieve high data rates for wireless communications either operating frequency should be increased or available bandwidth should increased hence, UWB is employed. Compared with the conventional communication system, UWB systems operates at very low emission power and high data rates are achieved over short distances. The FCC allocated 7.5 GHz bandwidth between 3.1 GHz and 10.6 GHz for unlicensed use of the commercial UWB systems [1]. The main purpose behind the designing of UWB antenna is to utilize the available unlicensed extremely high bandwidth which is present in microwave frequency spectrum.

The UWB in the 3.1 GHz-10.6 GHz band spectrum delivers data rates upto 400Mbps or more with availability in only a limited number of countries.

Main challenges in designing UWB antenna are requirement of compact size, impedance matching and feeding technique employed. Usually in UWB antennas the return losses have to remain below -10 dB over the wide frequency range. To carry out impedance matching successfully much efforts are needed, because of the small radiation resistance and large reactance values in this UWB range.

2.2 Literature Review to Achieve Wide Operating Bandwidth

UWB antenna technology is one of the advanced technology in this modern world [1]. FCC has approved 7.5 GHz bandwidth between 3.1 GHz and 10.6 GHz for the UWB communications [2]. Different types of UWB antennas have been proposed which include printed monopole antennas [3, 4, 5], single ended elliptical antennas [3]. Born a few decades ago, UWB has enabled the transmission of information over wide bandwidth, as a result special design considerations are being taken in the innovation of state of the art of UWB antennas. UWB antennas have contracted to a compact size which in turn affect the broadband response in terms of impedance, phase, gain, radiation patterns, VSWR etc.

2.3   Monopole Antennas

Conventional monopole has a straight wire configuration against a ground plane, as illustrated in Figure 2.1. It is one of the most widely used antennas for wireless communication systems due to its simple structure, low cost, omni-directional radiation patterns and ease for matching to $50\,\Omega$ [6]. Besides, it is unbalanced, thus eliminating the need for a balun, which may have a limited bandwidth [7].

The -10dB return loss bandwidth of straight wire monopole is typically around 10% 20%, depending on the radius-to-length ratio of the monopole.the bandwidth increases with the increase of the radius-to-length ratio. This indicates that a fatter structure will lead to a broader bandwidth because the current area and hence the radiation resistance are increased [8]. However, when the monopole radius is too large compared to the feeding line, the impedance mismatch between them will become significant and the bandwidth can not be further increased.
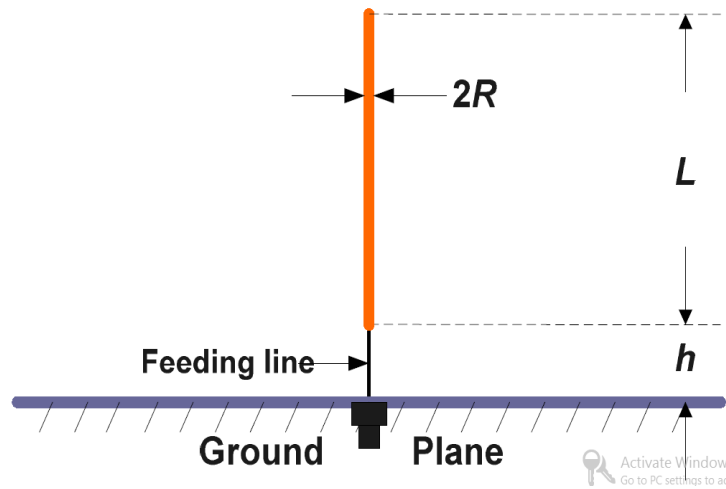
Figure 2.1: Geometry of straight wire monopole.

2.4   UWB Monopole antennas

For geometry of the monopole patch, Figure 2.2 presents several representative structures. These antennas achieve impedance bandwidth ratios from 2.3:1 to 3.8:1. Among various geometries of the monopole patches, the printed circular monopole antenna is one of the simplest [2, 9], which achieves the impedance bandwidth ratio of 3.8:1 (2.69 GHz   10.16 GHz) with satisfactory omni-directional radiation properties. Other monopoles such as octagon monopole [10], spline-shaped monopole [11], U-shaped monopole [12], knights helm shaped monopole [13] and two steps circular monopole [14], as shown in Figure 2.2, were also proposed and reviewed,. i.e., Ooi et al. [10] introduced the two-layer octagon monopole antenna based on the low-temperature co-fired ceramic (LTCC) technique, also obtaining an impedance bandwidth ratio of 3.8:1 (3.76 GHz 14.42 GHz). Lizzi et al. [11] proposed the spline-shaped monopole UWB antenna able to support multiple mobile wireless standards, covering DCS, PCS, UMTS, and ISM bands, with the bandwidth ratio of 2.3:1 (1.7 GHz   2.5 GHz).

For geometry of the ground plane, several representatives are also shown in Figure 2.3, and obtain

Figure 2.2: Various monopole antenna structures.

the impedance bandwidth ratios from 3.8:1 to more than 10:1. i.e., Huang et al. [15, 16] introduced an impedance matching technique by cutting a notch at the ground plane, and the impedance bandwidth can be enha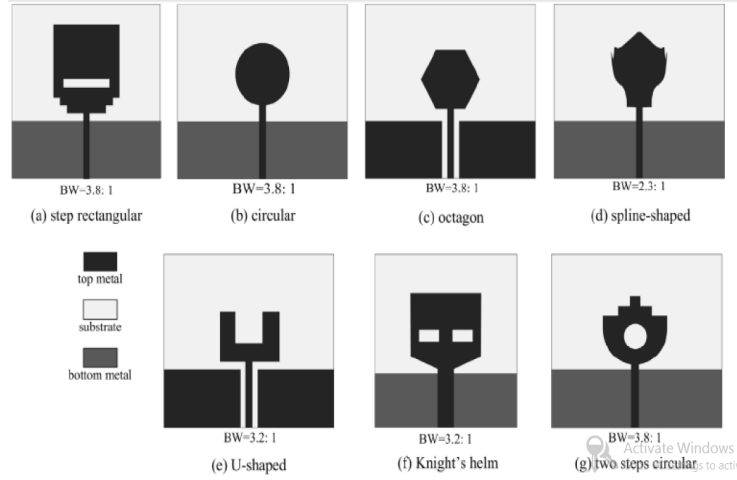nced by suitable size and position of the notch chosen. Azim et al. [17] proposed a method to improve the impedance bandwidth by cutting triangular shaped slots on the top edge of the ground plane. The printed square monopole antenna with symmetrical saw-tooth ground plane obtains the impedance bandwidth ratio of 5.5:1 (2.9 GHz   16GHz). Considering high concentration of currents in the corners of the patch or ground, Melo et al. [18] studied a rounded monopole patch with a rounded truncated ground plane. It provides an impedance bandwidth ratio of larger than 4.7:1 (2.55 GHz   12 GHz).
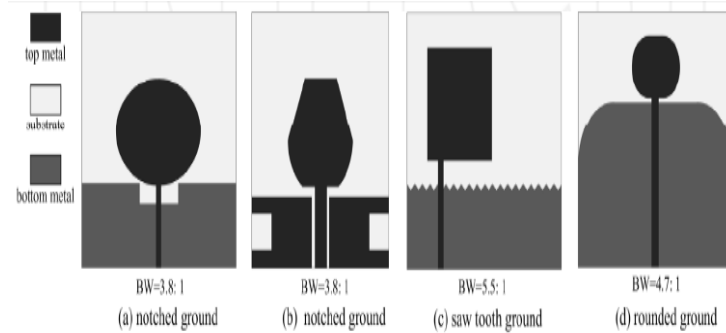
Figure 2.3: Various ground plane structures.

One of the interesting UWB printed monopole antenna designs is a trapezium ground plane with a rectangular patch monopole arose from the dis-cone antenna, where the rectangular patch is used to replace the disc, the trapeze-form ground plane is used to replace the cone, and the CPW is used to replace the coaxial feed, as shown in Figure 2.4 [19]. It is found that the printed rectangular antenna with a trapezium ground plane achieves an impedance bandwidth ratio of 5.1:1, which is similar to that of a dis-cone antenna. To enhance the bandwidth further, the input impedance is investigated by comparing bandwidths for various characteristics impedance of CPW feed-line. The impedance bandwidth ratio expands to 12:1 when the characteristic impedance of CPW feed-
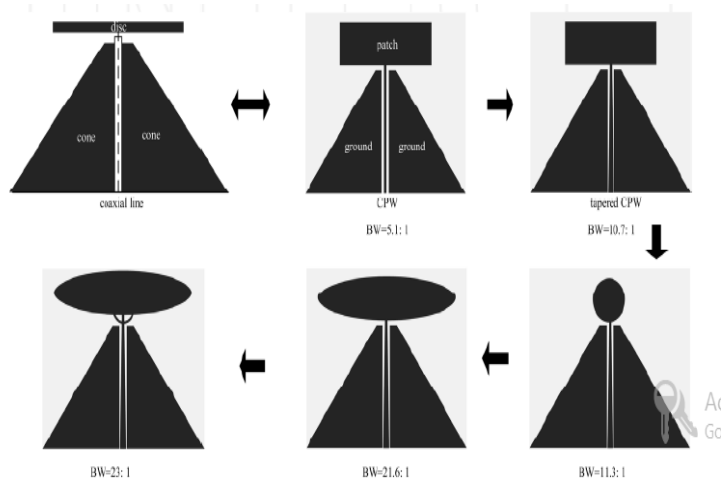
Figure 2.4: Various printed monopole antennas.

line is about 100, which means the impedance bandwidth is enhanced by a factor of about 2.3. In order to match $50\,\Omega$ SMA or N-type connectors, a linearly tapered central strip line is used as an impedance transformer and an impedance bandwidth ratio of 10.7:1 (0.76 GHz to 11 GHz) is obtained. Moreover, various printed monopoles and feed structures are also studied to enhance the bandwidth further [20, 21, 22, 23].

2.5   Advantages of UWB

UWB has a number of encouraging advantages that are the reasons why it presents a more eloquent solution to wireless broadband than other technologies. Firstly, according to Shannon-Hartley theorem, channel capacity is in proportion to bandwidth. Since UWB has an ultra wide frequency bandwidth, it can achieve huge capacity as high as hundreds of Mbps or even several Gbps with distances of 1 to 10 meters [24]. Secondly, UWB systems operate at extremely low power transmission levels. By dividing the power of the signal across a huge frequency spectrum, the effect upon any frequency is below the acceptable noise floor [25], as illustrated in Figure 2.5.

For example, 1 W of power spread across 1GHz of spectrum results in only 1 nW of power into each hertz band of frequency. Thus, UWB signals do not cause signicant interference to other wireless systems.

Thirdly, UWB provides high secure and high reliable communication solutions. Due to the low energy density, the UWB signal is noise-like, which makes unintended detection quite difficult. Furthermore, the noise-like signal has a particular shape; in contrast, real noise has no shape. For this reason, it is almost impossible for real noise to obliterate the pulse because interference would have to spread uniformly across the entire spectrum to obscure the pulse. Interference in only part of the spectrum reduces the amount of received signal, but the pulse still can be recovered to restore the signal. Hence UWB is perhaps the most secure means of wireless transmission ever previously available [8].
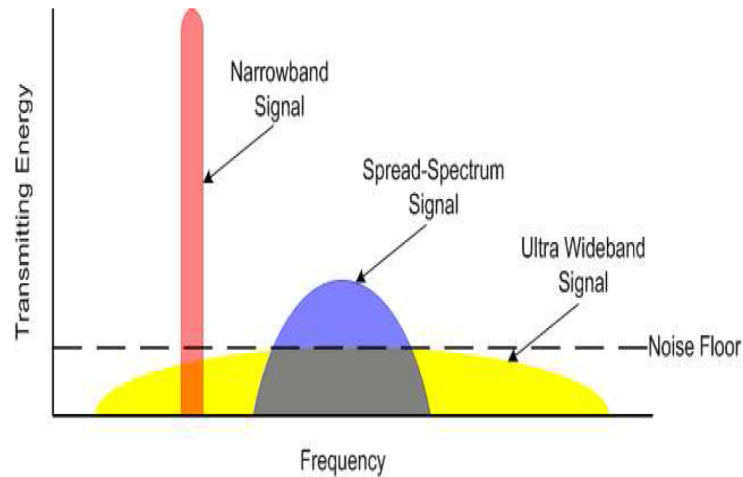
Figure 2.5: Ultra wideband communications spread transmitting energy across a wide spectrum of frequency

2.6 Applications

Due to its large operating bandwidth it is best suited for applications like high data rate wireless communications, imaging systems, high accuracy radars, health-care and personal entertainment few applications such as Satellite communications, Tactial communication for Electronic Warfare [26], networking, military area, mobile phones, wireless LAN, WPAN (Wireless Personal Area Network). In recent years, UWB radars sensors are used in medicine [27] and short range vehicular applications [28]. As mentioned earlier in this chapter, UWB offers some unique and distinctive properties that makes it attractive for various applications as shown in Figure 2.6. Firstly, UWB has the potential for very high data rates using very low power at very limited range, which will lead to the applications well suited for WPAN. The peripheral connectivity through cable-less connections to applications like storage, I/O devices and wireless USB will improve the ease and value of using Personal Computers (PCs) and laptops. High data rate transmissions between computers and consumer electronics like digital cameras, video cameras, MP3 players, televisions, personal video recorders, automobiles and DVD players will provide new experience in home and personal entertainment.

Secondly, sensors of all types also offer an opportunity for UWB to flourish [29]. Sensor networks is comprised of a large number of nodes within a geographical area. These nodes may be static, when applied for securing home, tracking and monitoring, or mobile, if equipped on soldiers, remen, automobiles, or robots in military and emergency response situations [30] The key requirements for sensor networks include low cost, low power and multi-functionality which can be well met by using UWB technology. High data rate UWB systems are capable of gathering and disseminating or exchanging a vast quantity of sensory data in a timely manner. The cost of installation and maintenance can drop significantly by using UWB sensor networks due to absence of wires. This merit is especially attractive in medical applications because a UWB sensor network frees the patient from being shackled by wires and cables when extensive medical monitoring is required. In addition, with a wireless solution, the coverage can be expanded more easily and can be more reliable.

Thirdly, positioning and tracking is another unique property of UWB. Because of the high data rate characteristic in short range, UWB provides an excellent solution for indoor location with a
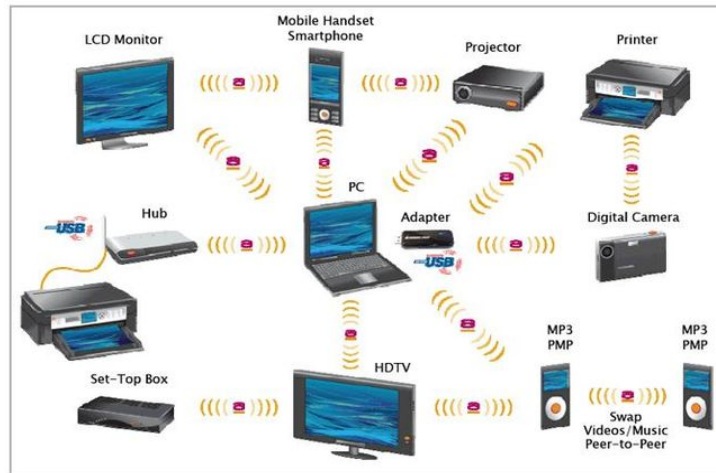
Figure 2.6: UWB Applications.

much higher degree of accuracy than a GPS. Furthermore, with advanced tracking mechanism, the precise determination of the tracking of moving objects within an indoor environment can be achieved with an accuracy of several centimeters [29]. UWB systems can operate in complex situations to yield faster and more effective communication between people. They can also be used to find people or objects in a variety of situations, such as casualties in a collapsed building after an earthquake, children lost in the mall, injured tourists in a remote area, fire fighters in a burning building and so on.

Lastly, UWB can also be applied to radar and imaging applications. It has been used in military applications to locate enemy objects behind walls and around corners in the battlefield. It has also found value in commercial use, such as rescue work where a UWB radar could detect a person's breath beneath rubble, or medical diagnostics where X-ray systems may be less desirable. UWB short pulses ensures very accurate delay estimates, enabling high definition radar. Based on the high ranging accuracy, intelligent collision-avoidance and cruise-control systems can be envisioned [30]. These systems can also improve airbag deployment and adapt suspension/braking systems depending on road conditions. Besides, UWB vehicular radar is also used to detect the location and movement of objects near a vehicle.

2.7 Swastika-Shaped Antenna

Most commonly used antennas in telecommunication are patch antennas, depending on the requirement of applications like operating frequency, directivity, polarization etc., the geometry of patch is modified accordingly. In patch antennas frequency of operation depends mainly on the thickness and electric permittivity of the substrate used. They are available at low-cost and can be fabricated easily. These patch antennas are fed by different types of feeding techniques like micro-strip feed, coaxial feed, coupled feed, aperture feed etc. [6] explains in detail about CPW-Fed UWB antenna. Generally micro-strip patch antennas have simple two-dimensional physical geometry so they are relatively inexpensive to design and manufacture.

Slot antennas are commonly used in the frequency range between 300MHz and 25GHz. The
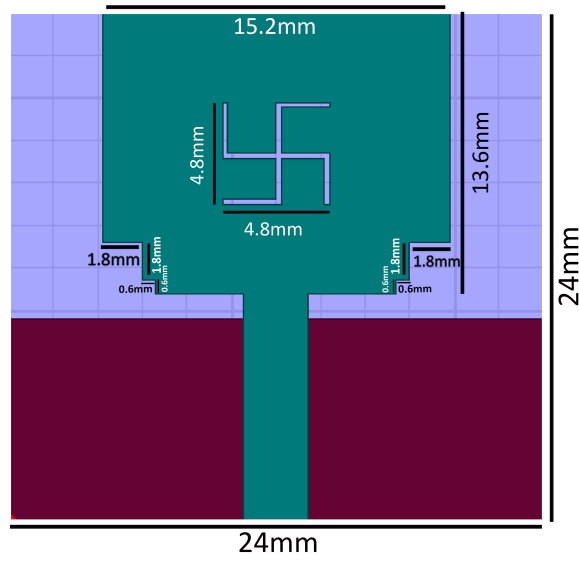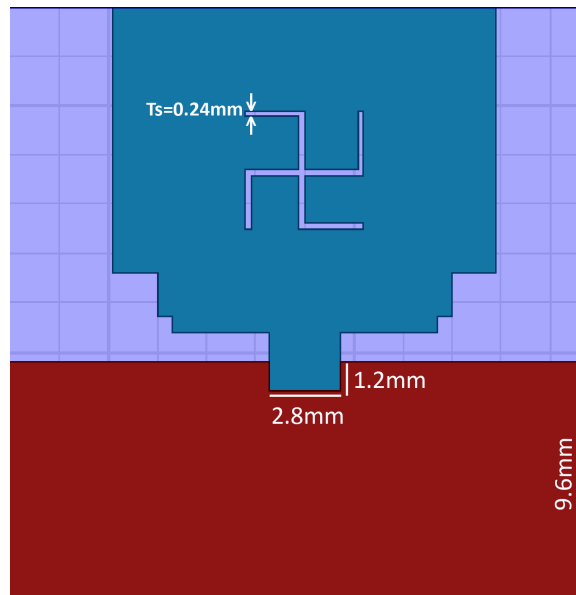
Figure 2.7: Swastika Slot Antenna Structure (a) Top view (b) Bottom view

length of the elongated slot in the basic slot-antenna is half of the wavelength which is cut in the conductive plane and placed at the center. From Babinets principle [31] this elongated slot behaves as resonant radiator. This principle was invented by Jacques Babinet, a French physicist and mathematician. This proposed principle relates the impedance and radiated fields of a slot antenna to that of field of a dipole antenna. The length and width of the slot determines the resonant frequency and bandwidth of slot radiator respectively. The slot antenna has a linear polarization. Basically both the slot antenna and dipole antenna have similar fields but their field components are interchanged, the dipole and slot will have vertical electrical field (E) and horizontal field (H) respectively [32]. The concept of making swastika slot in the radiating patch is to reduce the

conductance between rectangular patch and ground plane so that a small resistance can be capable of distributing the surface current along the symmetrical slot. Also swastika slot creates an equivalent circular symmetry which results in improve co-polarization and restricted cross polarization.

The geometry of Swastika Slot antenna shown in Figure 2.7 has a radiating patch above the substrate which has thickness of 1.385 mm and dimensions of 24 mm x 24 mm. The substrate is made up of material FR-4 which has relative dielectric constant and dielectric loss tangent of 4.4 and 0.0025 respectively.

There are two notches of each 1.8 mm x 1.8 mm and 0.6 mm x 0.6 mm at the bottom corners of radiating patch. They are basically provided for micro-strip feed impedance matching [33]. A ground plane with high conductivity is placed below the substrate. It consists of U-shaped slot of 2.8 mm x 1.2 mm dimensions. The ground plane has length of 9.6 mm. A swastika-shaped slot of dimensions 4.8 mm x 4.8 mm is embedded on the radiating patch. The width of each slot of swastika is Ts (0.24 mm). The impedance bandwidth is affected by the variation in the feed gap and height of the given substrate.

2.8 Swastika Slot Antenna with Concentric Circular Slots

In three antenna designs the swastika slot is surrounded by concentric circular slot. The circular slot width is varied by changing the radius of inner and outer circles. The width of circular slot is optimized for antennas to work in UWB range. These designs and their results are discussed below.

2.8.1 Antenna Design1 (Modified radiating patch)

In this design as shown in Figure 2.8, the dimension of swastika slot is same as that of normal swastika slot antenna. Here swastika is surrounded by a circular slot which has width of 0.1679 mm. The inner and outer radius of circular slot is 2.8519 mm and 3.019 mm respectively.
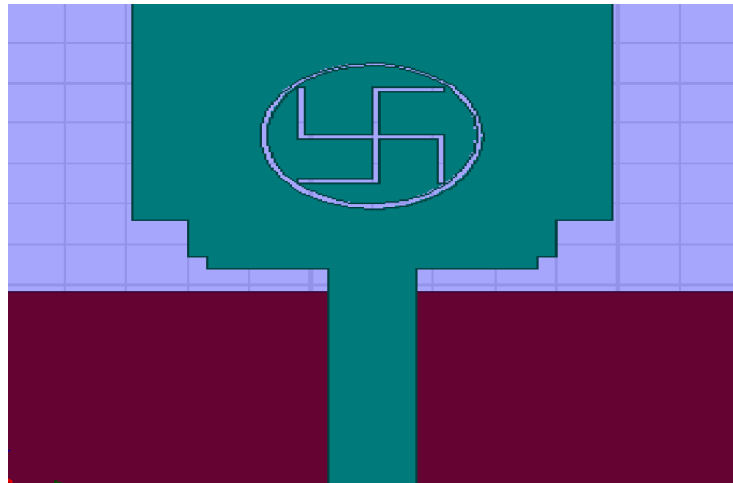
Figure 2.8: Geometry of Antenna Design 1.

Simulation Results: From Figure. 2.9 it can be observed that the antenna has a bandwidth of

7.1 GHz with return loss less than -10 dB from 3.7 GHz to 10.8 GHz. The minimum return loss obtained is -37.62dB at frequency of 9.1GHz
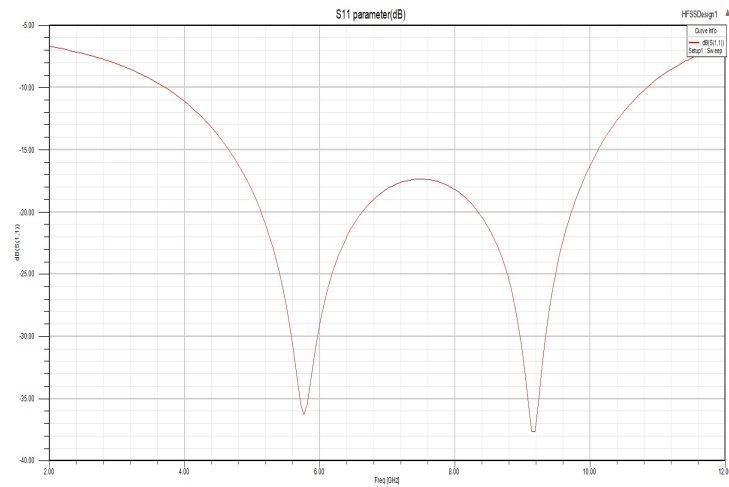
Figure 2.9: Return Loss of Antenna Design 1.

2.8.2 Antenna Design2 (Modified radiating patch)

In this design, the width of circular slot is increased to 1.367 mm as shown in Figure 2.10, by keeping inner circle radius same i.e 2.8519 mm and increasing the outer radius to 4.219 mm and rest of the dimensions are same as normal swastika slot antenna.
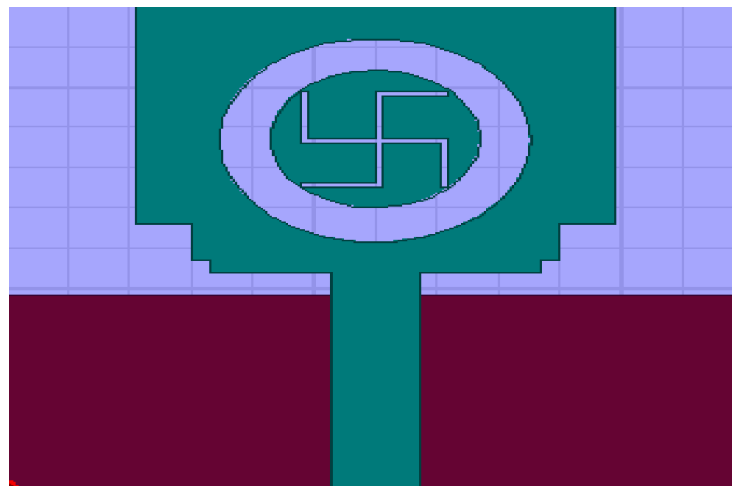
Figure 2.10: Geometry of Antenna Design 2.

Simulation Results: The bandwidth obtained for this antenna design is 7 GHz as defined for -10 dB return loss as shown in Figure 2.11. The lower and upper cut-off frequencies for -10 dB return loss are 3.6 GHz to 10.6 GHz. The minimum return loss in this 7GHz bandwidth is -35.6 dB at frequency 9.6 GHz.
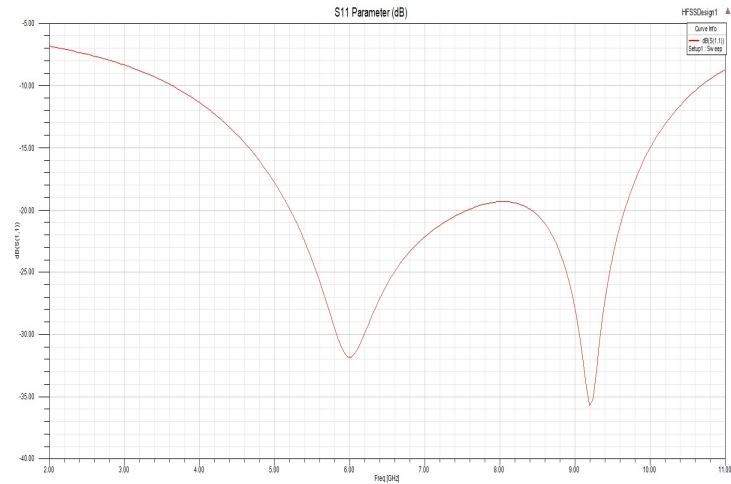
Figure 2.11: Return Loss of Antenna Design 2.

2.8.3 Antenna Design3 (Modified ground plane)

In Figure 2.12 antenna design 3 is shown, in which width of concentric circular slots is furthermore increased to 2.0679 mm. Here also inner circle radius is kept same as in antenna design 1, but outer circle radius is increased to 4.9198 mm.
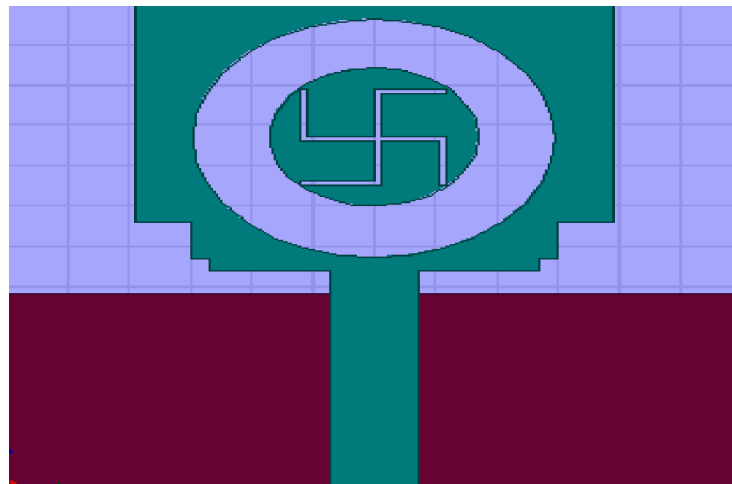
Figure 2.12: Geometry of Antenna Design 3.

Simulation Results: In Figure 2.13 return loss plot of antenna design 3 is obtained , which shows that this antenna covers a bandwidth of 6.72 GHz, from 3.78 GHz to 10.5 GHz with less than -10 dB return loss. The minimum return loss observed is -37.17 dB at frequency 6.3 GHz.
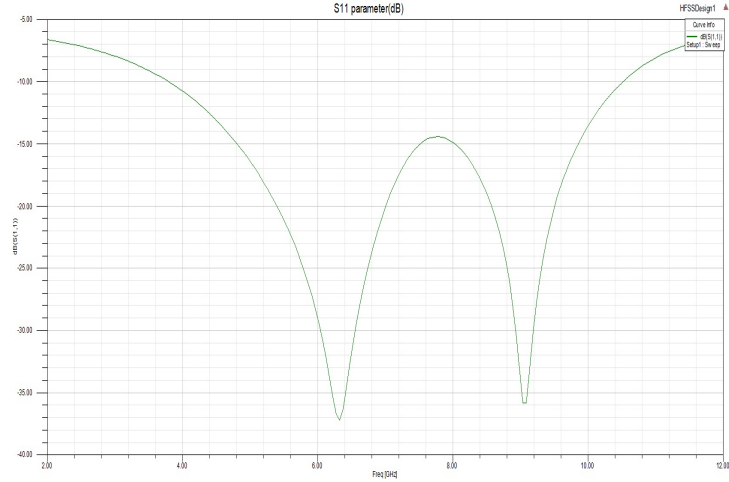
Figure 2.13: Return Loss of Antenna Design 3.

2.9 Swastika Slot Antenna with a Pair of Inverted L-shaped Slots on The Ground Plane

In this design the ground plane of swastika antenna is modified with a pair of inverted L-shaped slots. The dimension (a,b and c) and position of each L-shaped slot is mentioned in Figure 2.14.

These L-shaped slots are responsible for improving the bandwidth of this antenna. Impedance of this antenna is affected by the distribution of current density on the modified ground plane. The current density distribution is shown in Figure 2.15. The distance between these two inverted L-shaped slots found to be very crucial parameter, it should be large enough to minimize the coupling between each other. Surface current density in the middle area of the ground plane under micro-strip feed line changes with the change in distance between L-shaped slots.

Simulation Results: From Figure 2.16 It is observed that our proposed antenna design 4 covers a bandwidth of 6.9 GHz which ranges from 3.9 GHz to 10.8 GHz which clearly shows that it uses UWB efficiently. In this UWB the return losses are reduced and the minimum return loss obtained is -50.57dB at frequency 5.86 GHz.

2.10 Comparison of All Four Proposed Antenna Designs

It can be inferred from the comparison plot Figure 2.17 that over the UWB range the return losses are decreased in the proposed antennas as compared with the normal Swastika slot antenna and moreover return losses are reduced significantly in the frequency range from 8.2 GHz to 10.1 GHz.

This implies that the power losses are minimized. For all the antenna designs the bandwidth and minimum return losses obtained are tabulated in Table 2.1 . From Figure 2.18 it can be observed that the radiation patterns are almost similar in all the four antennas.
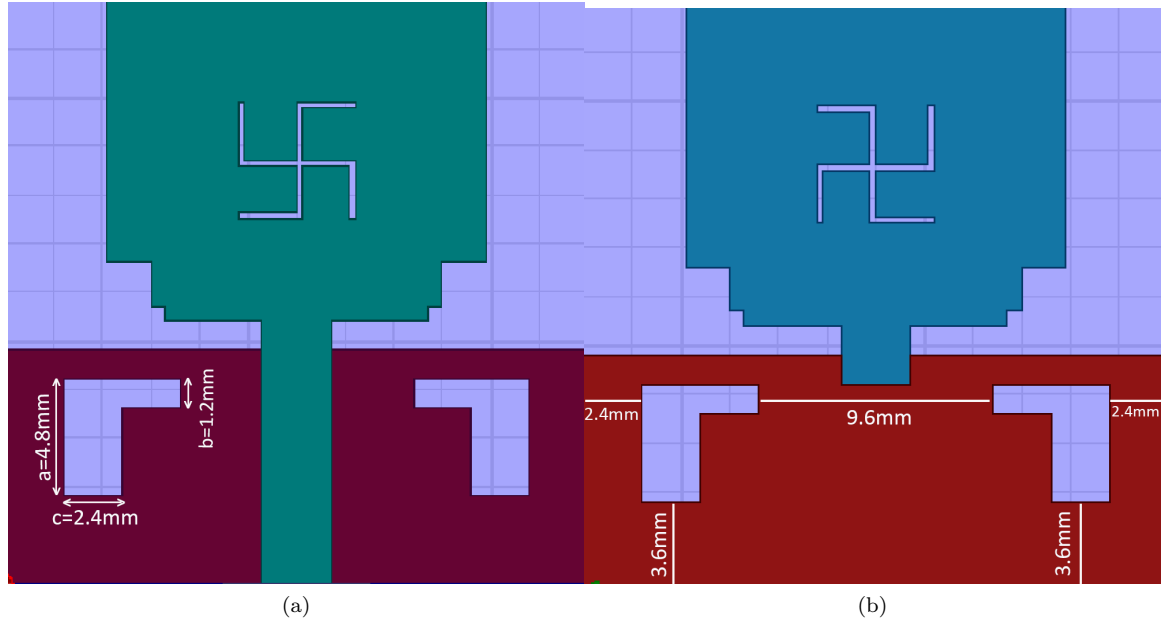
Figure 2.14: Geometry of Antenna Design 4 (a) Top view (b) Bottom view
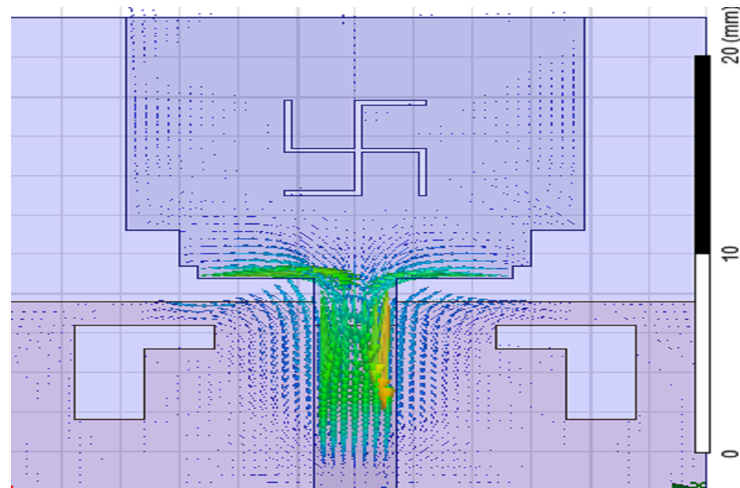
Figure 2.15: Current Distribution In Antenna Design 4.

2.11 Optimized UWB Tetraskelion-Shaped Slot Antenna with Notches

2.11.1 Optimization for Antenna Design 1

Figure 2.19 shows the geometry of Design 1 after optimization of antenna taken from [34]. The dimension of the substrate is 24 mm x 24 mm having thickness of 1.38 mm. FR-4 with relative dielectric constant tangent of 4.4 and dielectric loss tangent of 0.0025 is used as a material for the substrate. The length of the radiating patch is 15.2 mm x 13.2 mm. There is a ground plane opposite to the radiating patch. The length and width of the ground plane is 9.6 mm and 13.2 mm

(a)   (b)
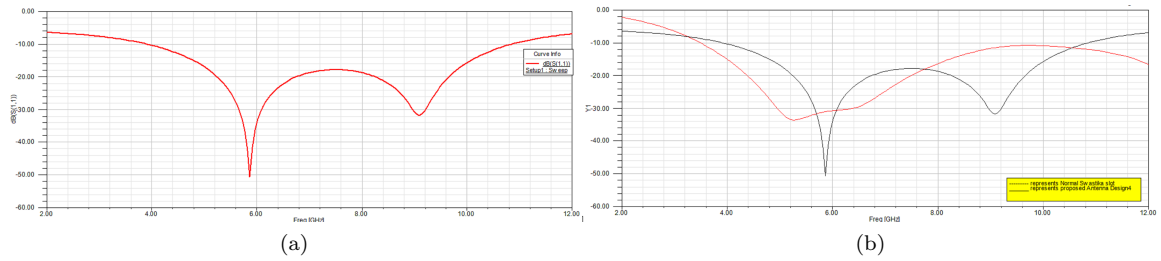
Figure 2.16: Return Loss (a): Design 4 (b): Comparison of Design 4 and Normal Swastika Antenna
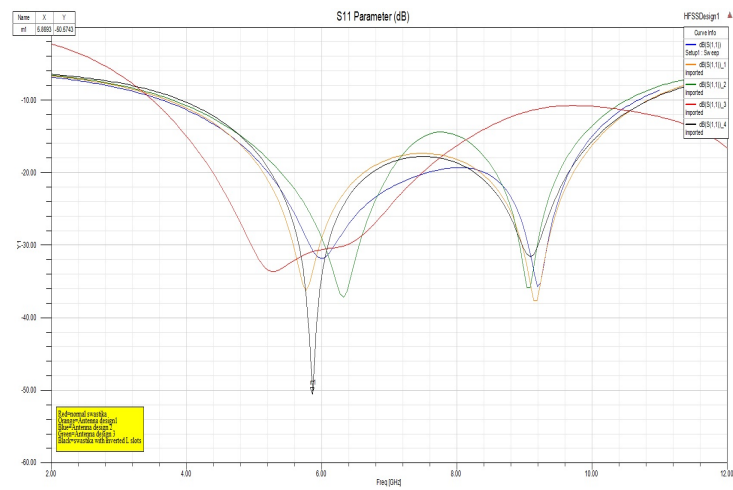
Figure 2.17: Comparison of bandwidth and return loses of normal Swastika slot antenna and proposed antenna designs

respectively. There are two slots on the ground plane, namely U-shaped slot and a pair of inverted L-shaped slots. The length and width of L and U shaped slots are 4.8 mm x 1.2 mm and 2.88 mm x 1.2 mm respectively. The dimension of the notches after the optimization are 1.8 mm x1.35 mm, 0.15 mm x 0.6 mm. In this design an additional circular notch is introduced of radius 0.4485 mm. These notches are necessary for matching the input impedance of micro-strip feed and variation of dimensions will affect the bandwidth and return losses. Figure 2.21 shows the geometry of normal tetraskelion shaped slot antenna with the variation in the dimensions of notches on the radiating patch. A tetraskelion shaped slot is embedded on the radiating patch, having dimensions of 4.8 mm x 4.8 mm and width of 0.24 mm.

15

(a) Design 1

(b) Design 2
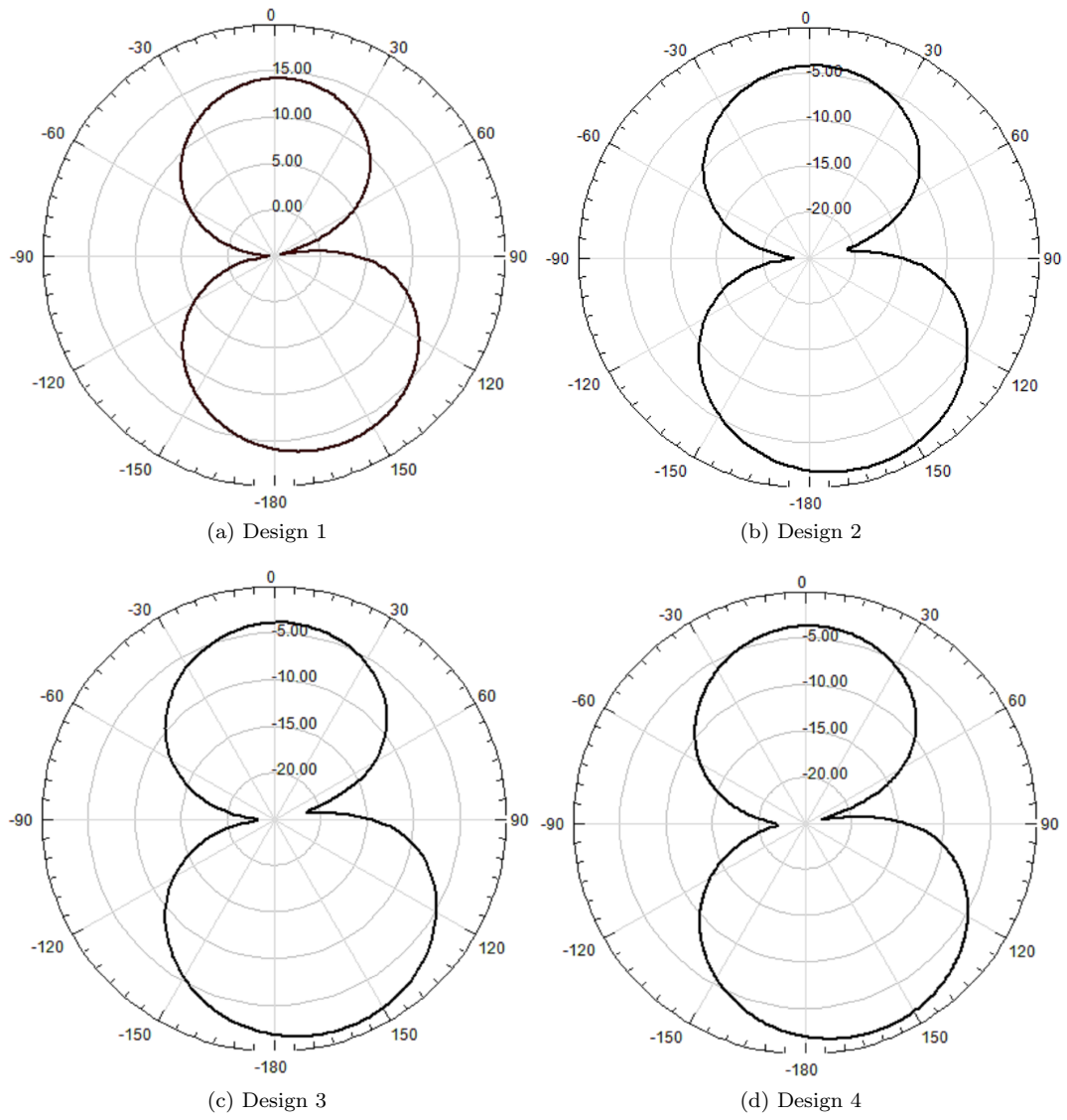
(c) Design 3

(d) Design 4

Figure 2.18: Radiation pattern of Antenna Designs 1,2,3,4

(a) Top View   (b) Bottom View
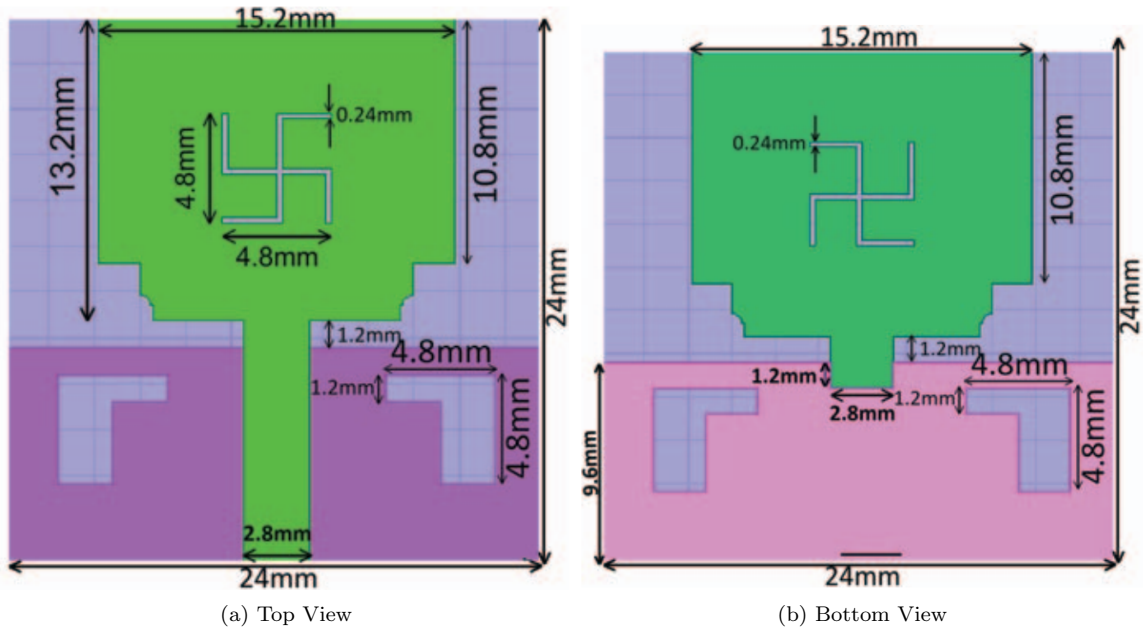
Figure 2.19: Tetraskelion-shaped slot antenna with Modified ground plane

(a)
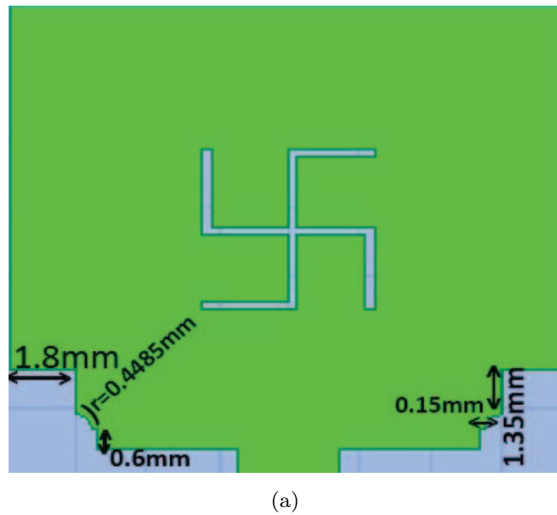
Figure 2.20: Dimensions of notches on the radiating patch i.e. Design F

Table 2.1: Tabular form of frequency of bandwidths and return losses

S.No	Slot Antenna Design	Bandwidth (less than -10dB)	Minimum Return Losses
1	Normal Swastika Slot Antenna	3.49 GHz-14.4 GHz	-37.8 dB
2	Antenna Design 1	3.7 GHz-10.8 GHz	-37.62 dB
3	Antenna Design 2	3.6 GHz-10.6 GHz	-35.6 dB
4	Antenna Design 3	3.78 GHz-10.5 GHz	-30.17 dB
5	Antenna Design 4	3.9 GHz-10.8 GHz	-50.57 dB

The variations in the dimensions of notches are tabulated in Table 2.2. In Figure 2.20 optimized version i.e. Design F.

2.11.2 Optimization for Antenna Design 2

Figure 2.21 shows the geometry of Design 2 with optimized dimensions of notches. The dimension of substrate and its material is same as in Design 1. In this design, radiating patch includes a circular slot of width 0.8 mm and ground plane has only U-shaped slot of dimension 1.2 mm x 2.8 mm. On the radiating patch their is concentric circular ring around the tetraskelion shaped slot. The radius of inner and outer circle slots is 2.91 mm and 3.71 mm respectively and the width of concentric circular ring is 0.8mm. Figure 2.22 shows the geometry of Design 2 with the variables a, b, c and d denoting the dimensions of notches.
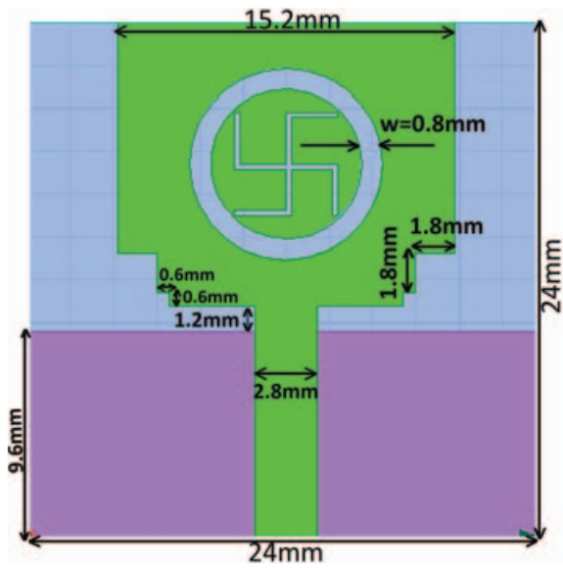
(a)

Figure 2.21: Tetraskelion shaped slot antenna with Modified radiating patch
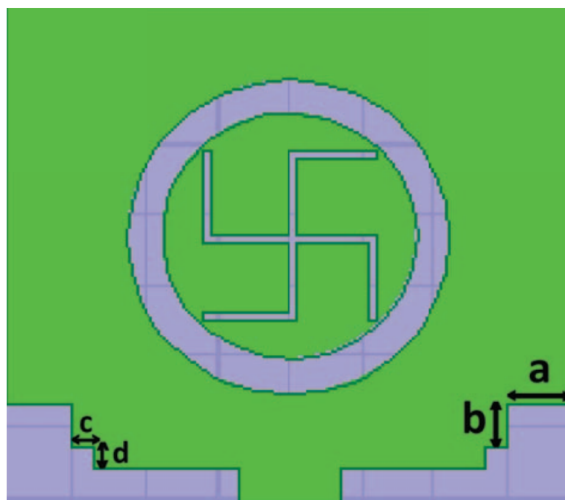
(a)

Figure 2.22: Variation of notches on Design 2

Table 2.2: DIMENSIONS OF NOTCHES FOR DESIGN 1

S.No	Design	a	b	c	d
1	Design A	-	-	-	-
2	Design B	-	-	2.4mm	0.6mm
3	Design C	1.8mm	0.6mm	0.6mm	0.6mm
4	Design D	1.8mm	1.2mm	0.6mm	0.6mm
5	Design E	1.8mm	1.8mm	0.6mm	0.6mm
6	Design F (optimized)	1.8mm	1.35mm	0.15mm	0.6mm

The Table 2.2 includes the variations in the dimension of notches a, b, c and d.

The above two optimized antenna designs as shown in Figure 2.19 and 2.21 are designed such that the return losses are minimized. Swastika slot is taken as reference since it is similar to a cross structure which exhibits circular symmetry [35, 36] and allows co-polarization.

Simulation Results:

The graphs and tables determine the variations in the bandwidth and return losses with the effect of notches for Design 1 and Design 2 respectively. Figure 2.23 and Figure 2.24 depicts the return losses and VSWR of all antennas with variation in dimensions of notches for Design 1 respectively. The minimum value of S11 parameter or the return losses are improved from -17.70 dB to - 61.30 dB. In order to know how much power is delivered to the antenna, Voltage Standing Wave Ratio (VSWR) is necessary to calculate. For good performance, VSWR should be less than 2. From the Figure 2.24 It can be observed that all the designs have VSWR $\leq$ 2.

From Figure 2.25 it is observed that the radiation pattern has small variations but the overall shape remains unchanged that means radiation pattern is not affected by varying the dimension of notches. The pattern is omni-directional which is one of the requirement of UWB antennas.

2.12   Conclusion

In this work four novel UWB slot antennas are proposed. All these antenna designs performed better than the normal Swastika slot antenna in terms of return loss, bandwidth and power loss. As the return losses are improved, the reduction in power loss is improved which is responsible for improvement of overall performance of antenna. These novel designs are utilizing almost full UWB range which makes this design very efficient. It can be observed that the impedance and radiation patterns are almost same in all the cases. Antenna design with a pair of inverted L-shaped slots performed better in terms of return loss, bandwidth and overall characteristics of antenna.
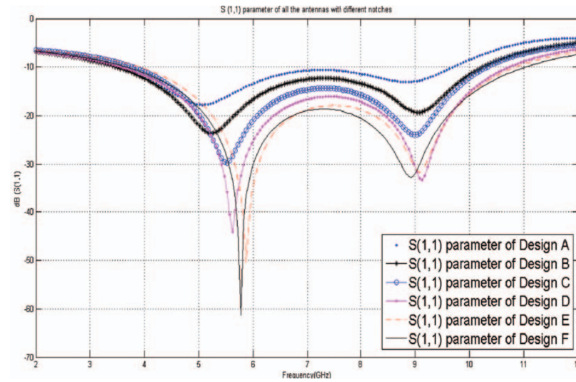
(a)

Figure 2.23: SS(1,1) parameter (return loss) with the variation of notches for Design 2
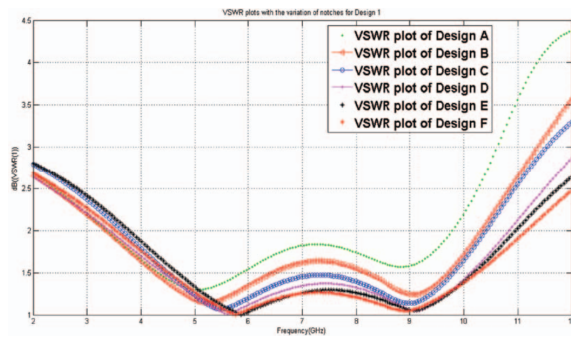
(a)

Figure 2.24: VSWR plots with the variation of notches for Design 2
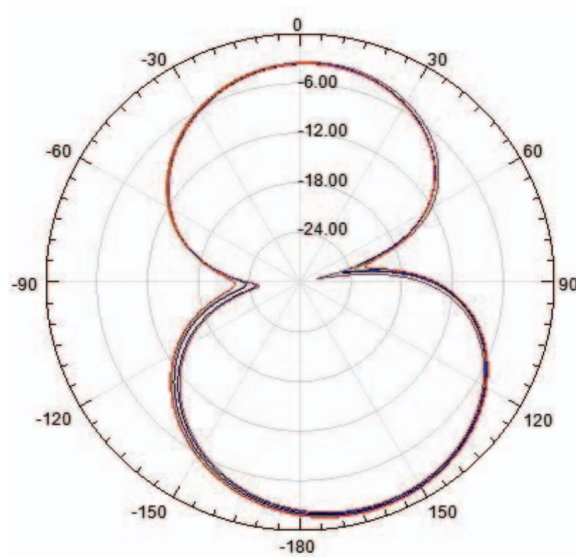
(a)

Figure 2.25: Radiation pattern with the variation of notches

21

Further, the effect of the notches on the radiating patch is studied and optimized. It can be noted that there are variations in bandwidth, return losses, radiation pattern and VSWR. It is observed that these two optimized antennas give better results. However radiation patterns obtained are same for both these antennas. The advantages of these optimized antennas are they are compact in size and work in the UWB range with reduced return losses and give best performance since very less amount of power is reflected from the antenna.

Chapter 3

Linear Dipole Antenna

3.1 Introduction

Wire antennas, linear geometry, are some of the oldest, simplest, cheapest, and in many cases the most versatile for many applications. The monopole and dipole antennas are commonly used for broadcasting, cellular phones, and wireless communications due to their Omni directive property. The flared section of transmission line is widely used as dipole antenna [6]. If l ¡ λ, the phase of the current standing wave pattern in each arm is the same throughout its length. In addition, spatially it is oriented in the same direction as that of the other arm as shown in Figure 3.1. Thus the fields radiated by the two arms of the dipole will primarily reinforce each other towards most directions of observation.
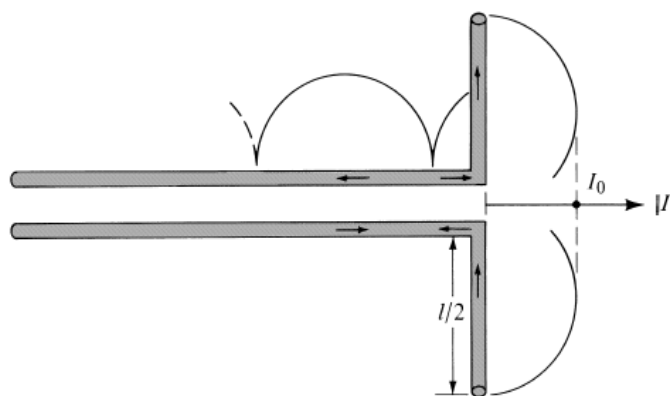
Figure 3.1: Current Distribution on Linear Dipole

If the diameter of each wire is very small the ideal standing wave pattern of the current along the arms of the dipole is sinusoidal with a null at the end. Because of its cyclical spatial variations, the current standing wave pattern of a dipole longer than λ undergoes 180 phase reversals between

adjoining half cycles. Therefore, the current in all parts of the dipole does not have the same phase. The fields radiated by some parts of the dipole will not reinforce those of the others. As a result, significant interference and canceling effects will be noted in the formation of the total radiation pattern. The dipole antennas whose length is even multiple of wavelength do not radiate since the fields radiated by one part cancel the field radiated by the other part.

3.2   Half Wave Dipole Antenna

The most commonly used dipole is the half wavelength dipole (/2-dipole). The half-wave dipole antenna is just a special case of the dipole antenna. The "half-wave" term means that the length of this dipole antenna is equal to a half-wavelength at the frequency of operation.

This antenna offers many advantages like

1. Reasonable size
2. Radiation pattern with single maximum
3. Manageable input impedance

A $\lambda/2$-dipole is shown in Figure 3.2 The $\lambda/2$-dipole dipole has impedance which can be easily matched to 50 ohms using impedance transformers.
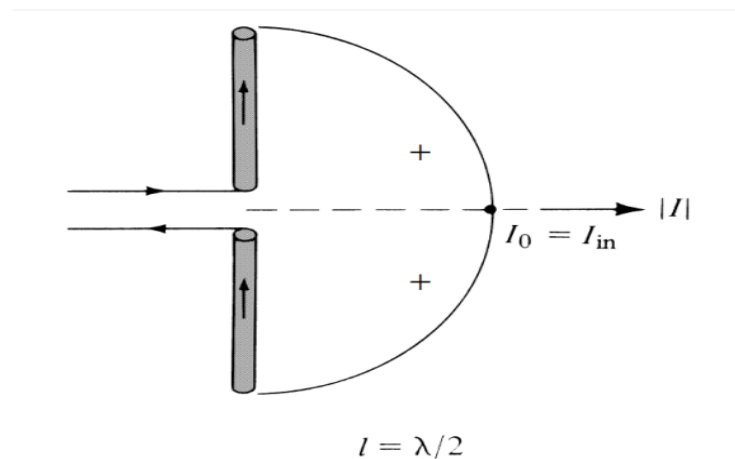
Figure 3.2: Current Distribution on Half-wave Dipole

3.3   Radiation Patterns

A radiation pattern defines the variation of the power radiated by an antenna as a function of the direction away from the antenna. Also known as Antenna Pattern or Far-Field Pattern. Radiation pattern of an antenna is graphical representation of radiated power at a fix distance from the antenna as a function of azimuth and elevation angle. So the antenna pattern gives information about the way in which the power is distributed in the space. For simplicity the radiation pattern can be drawn in 2D plane for different azimuth and elevation angle referred as azimuth plane pattern and elevation plane pattern. It is simpler to plot the radiation patterns in Cartesian (rectangular) coordinates,

especially when antenna radiation pattern consists of different side lobes and where these side lobes levels plays an important role. There are different types of antenna patterns described below.

3.3.1 Isotropic radiator

An Isotropic antenna has the radiations distributed uniformly in all direction. An isotropic antenna radiates all the power given. It is an imaginary antenna which does not exist practically. It is used as a reference to be compared with the other antennas.

3.3.2 Omnidirectional Antennas

Omnidirectional antenna can be referred as an antenna which has radiation pattern uniform and equally distributed in one plane generally referred to horizontal planes. Some applications like mobile, cell phones, FM radios, walkie-talkies, wireless computer networks, cordless phones, GPS, many portable handheld devices and in base stations antenna require with the characteristics that can radiate equally in a plane. Omnidirectional antenna has radiation pattern like doughnut shape. Slot antenna and dipole antenna, whip antenna, discone antenna, duck antenna are some good example of low gain omnidirectional antenna. Omnidirectional antenna with high gain can also be designed by narrowing the beamwidth of the antenna in the vertical plane will result in concentrating of energy in horizontal plane. Therefore, a narrow beamwidth antenna has a high gain and different type of omnidirectional antenna with various gains can be designed. A 0 dB gain antenna radiates more efficiently in vertical plane.

3.3.3 Directional Antennas

As the name suggest directional antennas concentrate their radiation in a particular direction. They are also known as Beam Antenna. They are useful in some point to point applications like satellite communication, in base station antenna to transmitting energy in a particular sector. Yagi, horn, log-periodic antenna and panel antenna are some examples that have directional radiation pattern.
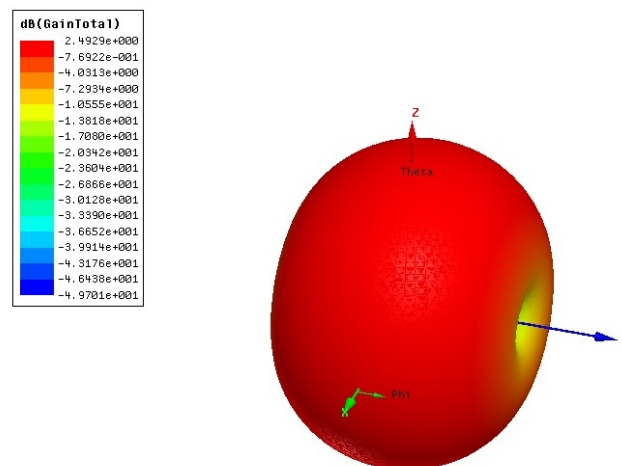
Figure 3.3: Radiation Pattern for Linear Horizontal Half-wave Dipole Antenna

3.4 Directivity

Directivity of an antenna shows that, how much the antenna is able to radiate in a particular given direction. It is a major requirement when antenna is working as a receiver. If an antenna radiates equally in all direction, then then the directivity of antenna is 1 or when measured with respect to isotropic antenna is 0dB. Directivity in its simple form can be described as the comparison of maximum radiation intensity to average radiation intensity. As

$$D = \frac{Maximum \quad Radiation \quad Intensity}{Average \quad Radiation \quad Intensity} \tag{3.1}$$

Directivity of an antenna with given angle shows that the antenna radiations are more concentrated in that given direction when talking about antenna at transmitting end. While in case of receiving antenna it will receive the power efficiently from the particular direction. The directivity of a half-wave dipole antenna is 1.64 (2.15 dB). The HPBW (Half power beam width) is the angular separation in which the magnitude of the radiation pattern decrease by 50

3.5 Antenna Gain

Antenna Gain is also referred as Power gain or simply Gain. This combines of antenna efficiency and directivity. For a transmitting antenna it shows how efficiently antenna is able to radiate the given power into space in a particular direction. While in case of receiving antenna it shows how well the antenna is to convert the received electromagnetic waves into electrical power. When it is calculated with efficiency and directivity D it is referred as Power Gain.

Power Gain = Efficiency * D

Efficiency of an antenna depends on the practical scenario and non-ideal conditions, which shows the performance of the antenna. In case of lossless antenna (efficiency=1), Gain is same as Directivity.

3.6 Bandwidth

Bandwidth describes the range of frequencies over which the antenna can properly radiate or receive energy. Often, the desired bandwidth is one of the determining parameters used to decide upon an antenna. For instance, many antenna types have very narrow bandwidths and cannot be used for wideband operation. Bandwidth is typically quoted in terms of VSWR (2:1). Alternatively, the Return loss $=20*\log10(0.2)=-13.98$ dB, typical value considered is -10 dB.

3.7   Antenna Polarization

Polarization of an antenna is polarization of the electromagnetic waves radiated from the antenna. Polarization on a wave is the orientation or path traces by the electric field vector as a function of time. Polarization can be categorized in three parts

a. Linear polarization

b. Circular polarization

c. Elliptical polarization

If the electric field vector of the wave at a given point in space follows a linear path, then the polarization is linear. Linear polarization is of two types Vertical and Horizontal. In case of circular and elliptical polarization electric field vector follows a circular and elliptical path. They can be Left hand polarized, if the electric field vector tracking the path by making clockwise rotation and Right hand polarized, if the vector tracking the path by making anti clockwise rotation. Linear dipole antenna is linearly polarized i.e, axial ratio value is infinity.

3.8   Radiation Resistance

Radiation resistance is that part of an antenna's feed point resistance that is caused by the radiation of electromagnetic waves from the antenna, as opposed to loss resistance (also called ohmic resistance) which generally causes the antenna to heat up. The total of radiation resistance and loss resistance is the electrical resistance of the antenna. The radiation resistance is determined by the geometry of the antenna, where loss resistance is primarily determined by the materials of which it is made. While the energy lost by ohmic resistance is converted to heat, the energy lost by radiation resistance is converted to electromagnetic radiation.

$$R = \frac{P}{I^2} \tag{3.2}$$

P is the power in the resulting electromagnetic field and I is the electric current flowing into the feeds of the antenna. This effective resistance is called Radiation resistance. If the dipole's length $(0.5*\lambda)$ is reduced to $0.48*\lambda$ the input impedance of the antenna becomes Zin = 70 Ohms, with no reactive component. This is a desirable property, and hence is often done in practice. The radiation pattern remains virtually the same. The above length is valid if the dipole is very thin. In practice, dipoles are often made with fatter or thicker material, which tends to increase the bandwidth of the antenna. When this is the case, the resonant length reduces slightly depending on the thickness of the dipole, but will often be close to $0.47*\lambda$.

Chapter 4

Antennas at Millimeter Wave Frequencies

4.1 Introduction

Though relatively new in the world of wireless communication, the history of millimeter wave technology goes back to the 1890s when J.C. Bose was experimenting with MM wave signals at just about the time when his contemporaries like Marconi were inventing radio communications. Following Boses research, MM wave technology remained within the confines of university and government laboratories for almost half a century. The technology started so see its early applications in Radio Astronomy in the 1960s, followed by applications in the military in the 70s. In the 80s, the development of MM wave integrated circuits created opportunities for mass manufacturing of MM wave products for commercial applications. In the 1990s, the advent of automotive collision avoidance radar at 77 GHz marked the first consumer oriented use of MM wave frequencies above 40 GHz. In 1995, the FCC opened the spectrum between 57 GHz and 64 GHz (commonly referred to as V-band or the 60GHz band) for unlicensed wireless communication (for US), resulting in the development of a plethora of broadband communication and radar equipment for commercial application. In 2003, the FCC authorized the use of 71-76 GHz and 81-86 GHz for licensed point-to-point communication, creating a fertile ground for new of industries developing products and services in this band.

MM wave generally corresponds to the radio spectrum between 30 GHz to 300 GHz, with wavelength between one and ten millimeters. However, in the context of wireless communication, the term generally corresponds to a few bands of spectrum near 38, 60 and 94 GHz, and more recently to a band between 70 GHz and 90 GHz (also referred to as E-Band), that have been allocated for the purpose of wireless communication in the public domain. MM wave frequencies are very promising for future wireless communication networks due to the massive amount of raw bandwidth and potential multigigabit-per-second (Gb/s) data rates [37, 38, 39]. Because of the availability of UWB of 7 GHz centred at 60 GHz. The communication at 60 GHz became great interest for the researchers and commercial vendors. Further in this thesis discussion about the problems, advantages and safety measures for 60 GHz wave propagation

4.2   Antenna centered at 60 GHz

There are other frequency bands and technologies that could compete in delivering data rates at 400Mbps or more, with discussion on standards for shorter-range high data rate solutions now beginning. Some examples include: UWB in the 3.1 GHz-10.6 GHz bandspectrum but with availability in only a limited number of countries; "higher order" modulation types to achieve higher data rates in limited lower frequency spectrum; or techniques like Dynamic Frequency Selection (DFS). Each has potential issues that must be resolved. Wireless connectivity trends have tended to track but lag wired solutions. With the increasing demand for higher data rates and more reliable service capabilities for wireless devices, wireless service providers are facing an unprecedented challenge to overcome a global bandwidth shortage. Early global activities on beyond fourth-generation (B4G) and fifth-generation (5G) wireless communication systems suggest that MM wave (mmWave) frequencies are very promising for future wireless communication networks due to the massive amount of raw bandwidth and potential multigigabit-per-second (Gb/s) data rates [40, 41, 42]. Both industry and academia have begun the exploration of the untapped mmWave frequency spectrum for future broadband mobile communication networks. This is due to the fact that many advantages can be found in operating such systems at MM waves compared to microwaves. First, because of the large available spectrum (7 GHz worldwide), very high data rates can be reached (up to 5 Gb/s). Second, it provides a high level of security and low interference with adjacent networks. Finally, compared to on-body devices operating at microwaves, the size of similar MM wave systems is significantly reduced.

Network interface cards operating at 1Gbps are now standard or available as an option in many new PC's and laptops. It is believed that as consumers grow accustomed to transferring files and other data at 1Gbps, they will also demand the option of doing so wireless.Antennas at 60 GHz have many advantages over other UWB available mentioned UWB which are dicussed below.

4.3   Disadvantages, Advantages and Safety Measures

MM wave at 60 GHz experiences a high order of attenuation while propagating in atmosphere. The main cause for this attenuation is because of oxygen and water content present in the atmosphere. MM waves are almost incapable to pass through the concrete walls because of the reduction in the signal strength, since a 15 cm thickness concrete walls offers -36 dB, of attenuation. Hence MM waves cannot propagate through concrete walls and therefore, long range communication is very difficult. These MM waves are best suited for Short-range (¡1km) wireless communication. It offers highly secure wireless communications with low interference from adjacent networks. MM waves at 60 GHz can make use of frequency reuse concept, the use of same frequency band in several local wireless communication systems. At MM wave frequencies, concern is more about skin and eyes as the small penetration depths prohibit propagation of energy further into the body. Under extreme environmental exposure harmful effects are and will be due to excessive absorption of energy, resulting in heating that can result in a detrimentally elevated temperature, such that at radiation levels low (less than 1nW/cm2) enough to avoid excessive heating it should be harmless [43, 44].

Ionizing Radiations like X-rays, UV-rays, and gamma rays can cause cancer. MM wave radiation

at 60 GHz, energy of photon (0.1 to 1.2 meV) is much lesser than the energy required to displace an electron from an atom (12 eV), hence it cannot be the cause for cancer and there are no other adverse health effects other than heating of tissue effect caused under extreme exposure.

4.4   Interactions of MM wave with Human Body

The primary biological targets of 60-GHz radiations are the skin and eyes. Exposure of the eyes leads to the absorption of the EM energy by the cornea characterized by a free water content of 75 % and a thickness of 0.5mm. Ocular lesions have been found after high-intensity exposure of the eye (3W/cm2, 6min) [45]. However, studies performed at 60 GHz (10mW/cm2, 8h) demonstrated no detectable physiological modifications [46], indicating that MM waves act on the cornea in a dose-dependent manner. Hereafter we will essentially consider the interactions with the skin as it covers 95 % of the human body surface. From the EM viewpoint, human skin can be considered as an anisotropic multilayer dispersive structure made of three different layers, namely, epidermis, dermis, and subcutaneous fat layer as shown in Figure 4.1. The skin also contains capillaries and nerve endings. It is mainly composed of 65.3 % of free water, 24.6 % of proteins, and 9.4 % of lipids [47].
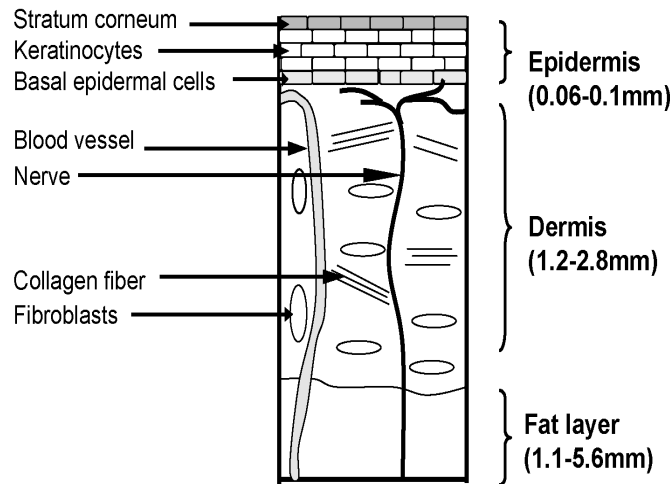
Figure 4.1: Schematic representation of the skin structure.

Knowledge of the dielectric properties of the skin is essential for the determination of the reflection from, transmission through, and absorption in the body, as well as for EM modeling. In contrast to frequencies below 20 GHz, existing data on the permittivity of tissues in the MM wave band are very limited [48, 49, 50, 51] due to some technical difficulties. Figure 4.2 provides summary of the data previously reported at 60 GHz.

4.5   Applications

MM wave BANs will also benefit civilian sectors such as healthcare, personal entertainment, sports training, and emergency services. Few of the applications shown in Figure 4.3 In hospital, clinics,

Reference	Complex permittivity ε^*	T, ℃	Method	Sample type
Gandhi *et al.* [8]	$8.89 - j13.15$	37 ± 0.5	E	*In vitro*
Alabaster *et al.* [9]	$9.9 - j9.0$	23	M	*In vitro*
Gabriel *et al.* [10] "wet skin"	$10.22 - j11.84$	37	E	*In vitro*
Gabriel *et al.* [10] "dry skin"	$7.98 - j10.90$	32.5 ± 0.5	E	*In vivo*
Alekseev *et al.* [11]	$8.12 - j11.14$	32.5 ± 0.3	M	*In vivo*
Chahat et al. [12]	$8.02 - j10.5$	32.5 ± 0.5	M	*In vivo*
Chahat *et al.* [13]	$8.4 - j10.96$	32.5 ± 0.5	M	*In vivo*

E=Extrapolation. M=Measurement. T=theoretical value.

Activate Windows

Figure 4.2: Summary of the data previously reported at 60 GHz.

entertainment venues, and public transport, there is a need to relay personalized data to and from individuals, in confined areas, or in crowds, and the high frequency and highly directive beams from small MM wave antennas will reduce interference between users and other communication equipment.

Various applications MM wave antennas have applications such as high definition video streaming,

Figure 4.3: Few 60 GHz applications: a) uncompressed video; b) office desktop; c) Fast downloading.

intelligent transport system (ITS), wireless gaming, mobile distributed computing, wireless gigabit Ethernet, health care, military and Airport security scanners.
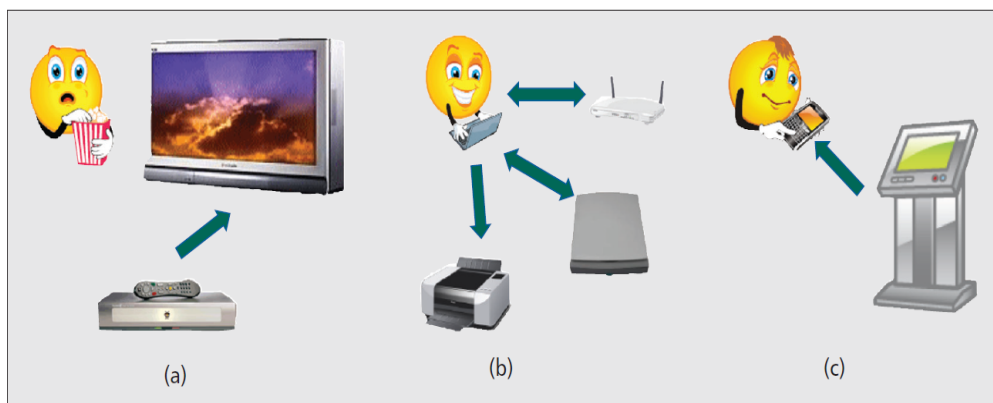
Chapter 5

A Compact Non-linear Millimeter Wave Antenna for UWB applications

5.1 Introduction

Owing to the increase in use of MM wave antenna, a non-linear wire dipole antenna is designed in this work. The antenna consists of two thin conducting arms of semi-circular shape of quarter wavelength each making overall antenna of half wavelength long. This antenna is designed to operate at 60 GHz which gives omni-directional pattern with the maximum gain at an elevation angle of 60°approximately. The bandwidth obtained covers almost entire unlicensed band available from 57 GHz to 64 GHz hence this antenna can be used for UWB applications as well. The curved structure of antenna enables it to be convenient to embroider on a fabric with reduced complexity in fabrication compared with the planar structures. This proposed antenna is analyzed to derive the expressions for the radiated fields and other antenna parameters like Directivity, Input and Radiation resistance, Radiation Intensity and Radiated Power. The theoretically derived results are plotted using MATLAB tool and to verify these theoretical results, the same antenna geometry is simulated using software HFSS.

5.2 Antenna Design and Analysis

The structure of dipole in shown in Figure 5.1. Two semi-circular arms are arranged to make non-linear geometry and is positioned symmetrically with respect to origin in YZ-plane. The radius of each semi-circular arm is selected in a manner such that total length of wire is half the wavelength. The geometry of two arms of the dipole and their respective tangents are defined by following vector expressions.
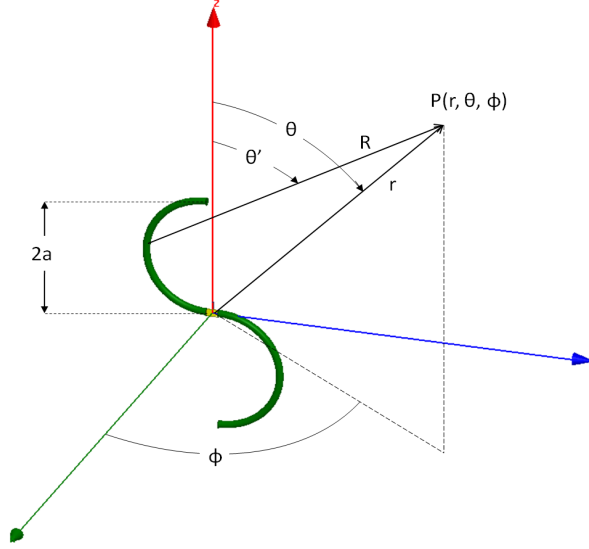
Figure 5.1: Proposed architecture of dipole.

$I^{st} - Arm$

$$l_1 = \hat{a}_y a \sin t + \hat{a}_z (a - a \cos t), \quad -\pi \leq t \leq 0$$

$$Tangent : \hat{t}_1 = \hat{a}_y \cos t + \hat{a}_z sint$$

$II^{nd} - Arm$

$$l_2 = \hat{a}_y a \sin t + \hat{a}_z (-a + a \cos t), \quad 0 \leq t \leq \pi$$

$$Tangent : \hat{t}_2 = \hat{a}_y \cos t - \hat{a}_y \sin t$$

$$(5.1)$$

Here a is radius of the semi-circular arc defined as $\frac{\lambda}{4\pi}$ where λ is wavelength for a half wavelength dipole. The geometry is parameterized by a parameter t which varies from $-\pi$ to π.

The current distribution on thin linear wire of different lengths are discussed in [6]. Current distribution on a thin linear dipole antenna can be approximated to sinusoidal distribution along its length. Hence the authors assumed that the current distribution along semi-circular dipole is sinusoidal and its direction is tangential to the curve. The expressions of current is

$$I_e = \begin{cases} I_0 \cos(kat)(\hat{a}_y \cos t + \hat{a}_z \sin t), & -\pi \leq t \leq 0 \\ \\ I_0 \cos(kat)(\hat{a}_y \cos t - \hat{a}_z \sin t), & 0 \leq t \leq \pi \end{cases} \qquad (5.2)$$

Where I_0 is peak value of current and $k = \frac{2\pi}{\lambda}$ is wave number. $\hat{a}_y$ and $\hat{a}_z$ are unit vectors along y and z axes. Current has no component along x-axis. It is assumed that the dipole antenna is center-fed and current is zero at the ends of antenna. This non-linear dipole is considered to be thin since its diameter is less than $\frac{\lambda}{10}$ and hence neglected in derivation to reduce mathematical complexity. Antenna parameters of proposed geometry are derived below.

33

5.2.1 Radiated Fields

To calculate the radiated fields, the two step procedure is used which is defined in [6]. In this procedure of fininding radiated fields first, Magnetic vector potential $\boldsymbol{A}$ is found and then Magnetic field $\boldsymbol{H}$ and Electric field $\boldsymbol{E}$ are calculated. The further analysis to obtain solutions of $\boldsymbol{H}$ and $\boldsymbol{E}$ field expressions is limited to far-field region only i.e. $kr \gg 1$. $\boldsymbol{A}$ can be calculated as,

$$A(x, y, z) = \frac{\mu}{4\pi} \int_c I_e(x', y', z') \frac{e^{-jkR}}{R} dl' \tag{5.3}$$

where I_e is source current, μ is permeability of medium and R is distance between observation point P(x,y,z) and any source point (x',y',z') as shown in Figure 5.1. These co-ordinates of source (primed) and observation (un-primed) are in rectangular co-ordinate systems.

$$R = \sqrt{(x - x')^2 + (y - y')^2 + (z - z')^2} \tag{5.4}$$

For simplicity source co-ordinates are parameterized by parameter t and observation point co-ordinates are expressed in spherical co-ordinate systems. Hence we have,

$$\begin{aligned} x' = 0, \quad y' = a\sin t, \quad z' = a - a\cos t, \qquad -\pi \le t \le 0 \\ x' = 0, \quad y' = a\sin t, \quad z' = -a + a\cos t, \qquad 0 \le t \le \pi \end{aligned} \tag{5.5}$$

$$\begin{aligned} x &= r\sin\theta\cos\phi \\ y &= r\sin\theta\sin\phi \\ z &= r\cos\theta \end{aligned} \tag{5.6}$$

Here (r, θ, ϕ) are co-ordinates of observation point in spherical co-ordinate system. For proposed geometry the expressions for R and dl' considering far field approximations reduces to the equations (7) and (8).

$$\begin{aligned} R &\approx r - a\sin\theta\sin\phi\sin t - a\cos\theta(1 - \cos t), & -\pi \le t \le 0 \\ R &\approx r - a\sin\theta\sin\phi\sin t + a\cos\theta(1 - \cos t), & 0 \le t \le \pi \end{aligned} \tag{5.7}$$

$$dl' = adt, \qquad\qquad -\pi \le t \le \pi \tag{5.8}$$

Since current I_e has components along y and z directions only, A_y and A_z components of magnetic vector potential $\boldsymbol{A}$ will exist along y and z directions respectively and A_x=0. It is difficult to find closed form solution for $\boldsymbol{A}$, so Simpson's $\frac{3}{8}^{th}$ rule [52] is used to numerically compute the integration. For simplicity the A_y and A_z components are again divided into two part. The detailed derivation is as follows:

$$A_y = \frac{\mu}{4\pi} \left(\int_{-\pi}^{0} I_0 \cos(kat) \cos t \frac{e^{-jkR}}{R} adt \quad + \int_0^{\pi} I_0 \cos(kat) \cos t \frac{e^{-jkR}}{R} adt \right) \tag{5.9}$$

For the ease in calculations this integral equation (9) is split into two parts as given below.

$$A_y = A_{y1} + A_{y2} \tag{5.10}$$

Now each integration is calculated separately. A_{y1} is expressed using equations (7) and (8) as,

$$A_{y1} = \frac{\mu a I_0 e^{-jkr}}{4\pi r} \int\limits_{-\pi}^{0} \left(\cos(kat)\cos t \quad \times exp\Big\{ jka(\sin t \sin\theta\sin\phi + \cos\theta(1-\cos t))\Big\} \right) dt \qquad (5.11)$$

Using Simpson's $\frac{3}{8}^{th}$ rule,

$$A_{y1} = \frac{3\mu a I_0 e^{-jkr}}{128r} \left(\sqrt{3}e^{\frac{-jka}{2}(\sqrt{3}\sin\theta\sin\phi-\cos\theta)} - e^{\frac{-jka}{2}(\sqrt{3}\sin\theta\sin\phi-3\cos\theta)} + \frac{4}{3} \right) \qquad (5.12)$$

A_{y2} is calculated in similar manner as A_{y1}.

$$A_{y2} = \frac{\mu a I_0 e^{-jkr}}{4\pi r} \int\limits_{0}^{\pi} \left(\cos(kat)\cos t \quad \times exp\Big\{ jka(\sin t \sin\theta\sin\phi \quad - \cos\theta(1-\cos t))\Big\} \right) dt \qquad (5.13)$$

$$A_{y2} = \frac{3\mu a I_0 e^{-jkr}}{128r} \left(\sqrt{3}e^{\frac{jka}{2}(\sqrt{3}\sin\theta\sin\phi-\cos\theta)} - e^{\frac{jka}{2}(\sqrt{3}\sin\theta\sin\phi-3\cos\theta)} + \frac{4}{3} \right) \qquad (5.14)$$

Hence A_y from equation (12) and (14) can be written as

$$A_y = \frac{3\mu a I_0 e^{-jkr}}{64r} \times \left(\sqrt{3}\cos\left(\frac{ka(\sqrt{3}\sin\theta\sin\phi - \cos\theta)}{2} \right) - \cos\left(\frac{ka(\sqrt{3}\sin\theta\sin\phi - 3\cos\theta)}{2} \right) + \frac{4}{3} \right)$$
$$(5.15)$$

In similar way as A_y, A_z is also calculated.

$$A_z = \frac{\mu}{4\pi} \left(\int\limits_{-\pi}^{0} I_0 \cos(kat)\sin t \frac{e^{-jkR}}{R} a dt - \int\limits_{0}^{\pi} I_0 \cos(kat)\sin t \frac{e^{-jkR}}{R} a dt \right) \qquad (5.16)$$

Splitting the above equation in two parts and using equations (7) and (8), individual parts A_{z1} and A_{z2} are given as,

$$A_z = A_{z1} + A_{z2} \qquad (5.17)$$

$$A_{z1} = \frac{\mu a I_0 e^{-jkr}}{4\pi r} \int\limits_{-\pi}^{0} \left(\cos(kat)\sin t \quad \times exp\Big\{ jka(\sin t \sin\theta\sin\phi \quad + \cos\theta(1-\cos t))\Big\} \right) dt \qquad (5.18)$$

$$A_{z1} = -\frac{3\mu a I_0 e^{-jkr}}{128r} \left(\sqrt{3}e^{\frac{-jka}{2}(\sqrt{3}\sin\theta\sin\phi-3\cos\theta)} + 3e^{\frac{-jka}{2}(\sqrt{3}\sin\theta\sin\phi-\cos\theta)} \right) \qquad (5.19)$$

$$A_{z2} = -\frac{\mu a I_0 e^{-jkr}}{4\pi r} \int\limits_{0}^{\pi} \left(\cos(kat)\sin t \times exp\Big\{ jka(\sin t \sin\theta\sin\phi - \cos\theta(1-\cos t))\Big\} \right) dt \qquad (5.20)$$

$$A_{z2} = -\frac{3\mu a I_0 e^{-jkr}}{128r}\left(\sqrt{3}e^{\frac{jka}{2}(\sqrt{3}\sin\theta\sin\phi - 3\cos\theta)} + 3e^{\frac{jka}{2}(\sqrt{3}\sin\theta\sin\phi - \cos\theta)}\right) \tag{5.21}$$

The final expression for A_z from equation (19) and (21) is,

$$A_z = -\frac{3\mu a I_0 e^{-jkr}}{64r}\times\left(\sqrt{3}\cos\left(\frac{ka(\sqrt{3}\sin\theta\sin\phi - 3\cos\theta)}{2}\right) + 3\cos\left(\frac{ka(\sqrt{3}\sin\theta\sin\phi - \cos\theta)}{2}\right)\right) \tag{5.22}$$

Transforming from rectangular to spherical components,

$$A_r = A_y\sin\theta\sin\phi + A_z\cos\theta$$

$$A_\theta = A_y\cos\theta\sin\phi - A_z\sin\theta \tag{5.23}$$

$$A_\phi = A_y\cos\phi$$

Hence expressions for A_r, A_θ and A_ϕ can be written as

$$A_r = C\left(\left(\sqrt{3}\cos\left(kaf_2\right) - \cos\left(kaf_1\right) + \frac{4}{3}\right)\sin\theta\sin\phi - \left(\sqrt{3}\cos\left(kaf_1\right) + 3\cos\left(kaf_2\right)\right)\cos\theta\right) \tag{5.24}$$

$$A_\theta = C\left(\left(\sqrt{3}\cos\left(kaf_2\right) - \cos\left(kaf_1\right) + \tfrac{4}{3}\right)\cos\theta\sin\phi + \left(\sqrt{3}\cos\left(kaf_1\right) + 3\cos\left(kaf_2\right)\right)\sin\theta\right) \tag{5.25}$$

$$A_\phi = C\left(\sqrt{3}\cos\left(kaf_2\right) - \cos\left(kaf_1\right) + \frac{4}{3}\right)\cos\phi \tag{5.26}$$

where expressions for C, f_1 and f_2 are given by

$$f_1(\theta,\phi) = \frac{\sqrt{3}\sin\theta\sin\phi - 3\cos\theta}{2} \tag{5.27}$$

$$f_2(\theta,\phi) = \frac{\sqrt{3}\sin\theta\sin\phi - \cos\theta}{2} \tag{5.28}$$

$$C = \frac{3\mu a I_0 e^{-jkr}}{64r} \tag{5.29}$$

$\boldsymbol{H}$ fields can be calculated using below equation [?]

$$H = \frac{1}{\mu}\left(\nabla\times A\right) \tag{5.30}$$

$\boldsymbol{H}$ can be defined in spherical co-ordinate system which has three components H_r, H_θ, H_ϕ along r, θ and ϕ direction respectively. In far field region, since $r \gg \lambda$, $1/r^n$ terms for n $\geq$ 2 can be neglected.

Final expressions for H_r, H_θ, H_ϕ can be approximated to,

$$H_r \approx 0 \tag{5.31}$$

$$H_\theta \approx j\frac{3kaI_0 e^{-jkr}}{64r} \times \left(\sqrt{3}\cos\left(kaf_2\right) - \cos\left(kaf_1\right) + \frac{4}{3}\right)\cos\phi \tag{5.32}$$

$$H_\phi \approx -j\frac{3kaI_0 e^{-jkr}}{64r} \times \left(\left(\sqrt{3}\cos\left(kaf_2\right) - \cos\left(kaf_1\right) + \frac{4}{3}\right)\cos\theta\sin\phi + \left(\sqrt{3}\cos\left(kaf_1\right) + 3\cos\left(kaf_2\right)\right)\sin\theta\right) \tag{5.33}$$

E fields are obtained by using equation

$$E = \frac{1}{j\omega\varepsilon}\nabla \times H \tag{5.34}$$

Below E_r, E_θ, E_ϕ components are evaluated by considering far field approximations.

$$E_r \approx 0 \tag{5.35}$$

$$E_\theta \approx -j\eta k\frac{3aI_0 e^{-jkr}}{64r} \times \left(\left(\sqrt{3}\cos\left(kaf_2\right) - \cos\left(kaf_1\right) + \frac{4}{3}\right)\cos\theta\sin\phi + \left(\sqrt{3}\cos\left(kaf_1\right) + 3\cos\left(kaf_2\right)\right)\sin\theta\right) \tag{5.36}$$

$$E_\phi \approx -j\eta k\frac{3aI_0 e^{-jkr}}{64r} \times \left(\sqrt{3}\cos\left(kaf_2\right) - \cos\left(kaf_1\right) + \frac{4}{3}\right)\cos\phi \tag{5.37}$$

The magnitude of total electric field is given by following equation.

$$E_T = \sqrt{{E_\phi}^2 + {E_\theta}^2} \tag{5.38}$$

5.2.2   Power density, Radiation Intensity

As per the definition given in [?] average Poynting vector for a dipole is written as,

$$W_{av} = \tfrac{1}{2}\mathrm{Re}\left[E \times H^*\right] = \tfrac{1}{2}\mathrm{Re}\left[\hat{a}_r\left(E_\theta H_\phi^* - E_\phi H_\theta^*\right)\right]$$

$$W_{av} = \tfrac{\hat{a}_r}{2\eta}\left[|E_\theta|^2 + |E_\phi|^2\right] \tag{5.39}$$

37

So,

$$W_{av} = \frac{\hat{a}_r \eta}{2} \left(\frac{3kaI_0}{64r} \right)^2 \times \left(\left(\left(\sqrt{3} \cos\left(kaf_2 \right) - \cos\left(kaf_1 \right) + \frac{4}{3} \right) \cos\theta \sin\phi + \left(\sqrt{3} \cos\left(kaf_1 \right) + 3\cos\left(kaf_2 \right) \right) \sin\theta \right)^2 \right.$$
$$\left. + \left(\left(\sqrt{3} \cos\left(kaf_2 \right) - \cos\left(kaf_1 \right) + \frac{4}{3} \right) \cos\phi \right)^2 \right)$$

(5.40)

and hence Radiation Intensity as

$$U = r^2 W_{av}$$

$$U = \frac{a_r \eta}{2} \left(\frac{3kaI_0}{64} \right)^2 \times \left(\left(\left(\sqrt{3} \cos\left(kaf_2 \right) - \cos\left(kaf_1 \right) + \frac{4}{3} \right) \cos\theta \sin\phi + \left(\sqrt{3} \cos\left(kaf_1 \right) + 3\cos\left(kaf_2 \right) \right) \sin\theta \right)^2 \right.$$
$$\left. + \left(\left(\sqrt{3} \cos\left(kaf_2 \right) - \cos\left(kaf_1 \right) + \frac{4}{3} \right) \cos\phi \right)^2 \right)$$

(5.41)

Power radiated is found by integrating average Poynting vector over a sphere of radius r.

$$P_{rad} = \int\limits_{\phi=0}^{2\pi} \int\limits_{\theta=0}^{\pi} W_{av} \cdot \hat{a}_r r^2 \sin\theta d\theta d\phi$$

(5.42)

$$P_{rad} = \frac{\eta}{2} \left| I_0 \right|^2 \left(\frac{3ka}{64} \right)^2 \left(C_1 \right)$$

(5.43)

where C_1 is defined by the equation,

$$C_1 = \int\limits_{\phi=0}^{2\pi} \int\limits_{\theta=0}^{\pi} \left(\left(\left(\sqrt{3} \cos\left(kaf_2 \right) - \cos\left(kaf_1 \right) + \frac{4}{3} \right) \times \cos\theta \sin\phi \right. \right.$$
$$\left. + \left(\sqrt{3} \cos\left(kaf_1 \right) + 3\cos\left(kaf_2 \right) \right) \sin\theta \right)^2 + \left(\left(\sqrt{3} \cos\left(kaf_2 \right) - \cos\left(kaf_1 \right) + \frac{4}{3} \right) \cos\phi \right)^2 \right)$$

(5.44)

Finding value of C_1 using Simpson's $\frac{3}{8}^{th}$ rule ,

$$C_1 \approx 202.28$$

(5.45)

The units of each parameter are given below:
W_{av}= Watt per square metre
U = Watt per unit solid angle
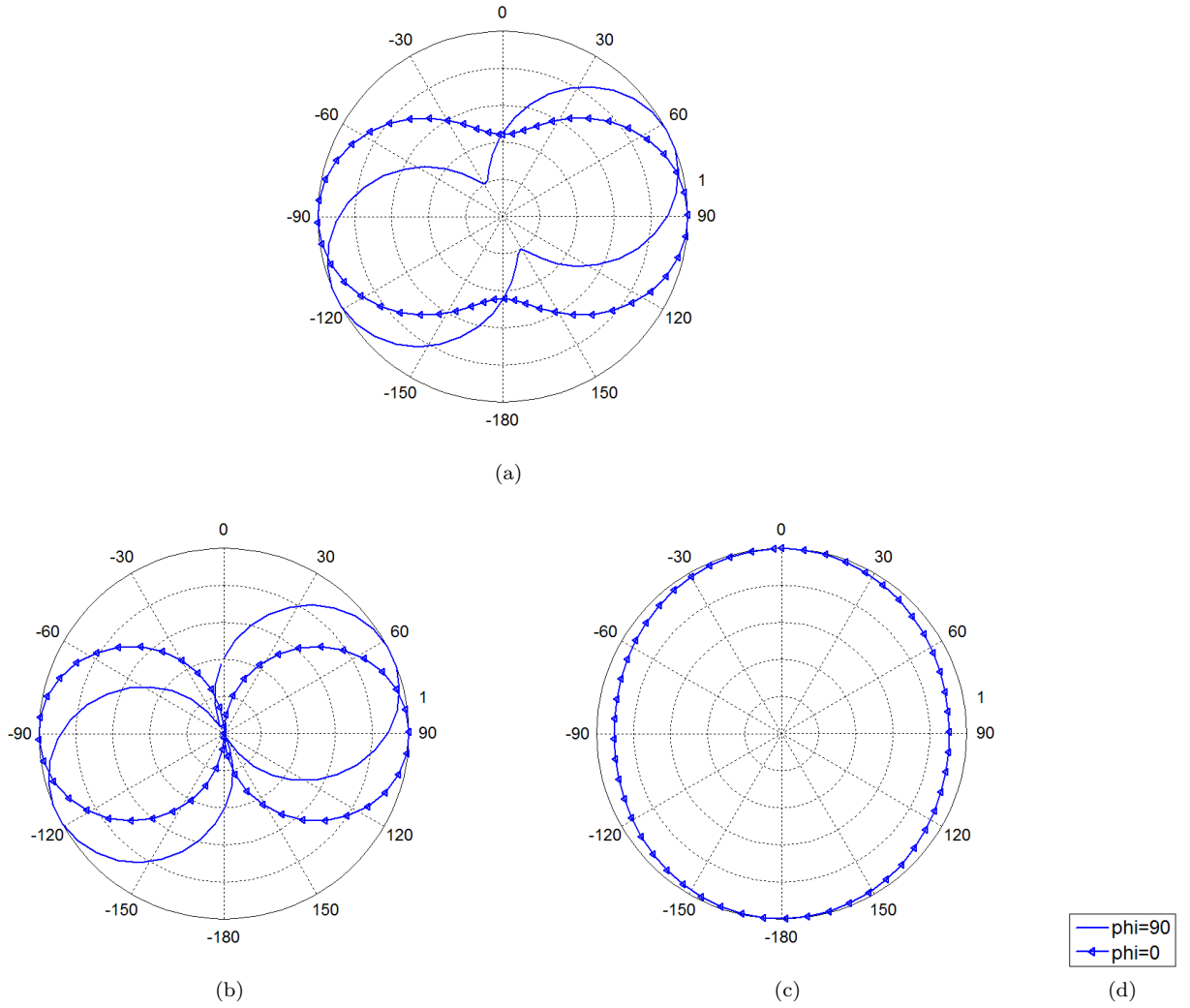P_{rad}= Watt

(a)

(b)   (c)   (d)

Figure 5.2: Radiation Pattern plotted using matlab (a) E_T, (b) E_θ, (c) E_ϕ

5.2.3   Directivity

Directivity of an antenna can be defined as ratio of radiation intensity in a given direction to the radiation intensity averaged over all directions. Hence its expression can be written as,

$$D_0 = \frac{U}{U_0}$$

$$D_{max} = 4\pi \frac{U_{\max}}{P_{rad}}$$

(5.46)

where,

U_{max} is maximum radiation intensity in Watt/unit solid angle and P_{rad} is power radiated in Watt. Directivity is a dimensionless quantity.

For the proposed antenna the direction of maximum radiation intensity is at an elevation angle

39

of 60°. Directivity of proposed antenna reduces to,

$$D_0 \approx 1.66 \tag{5.47}$$
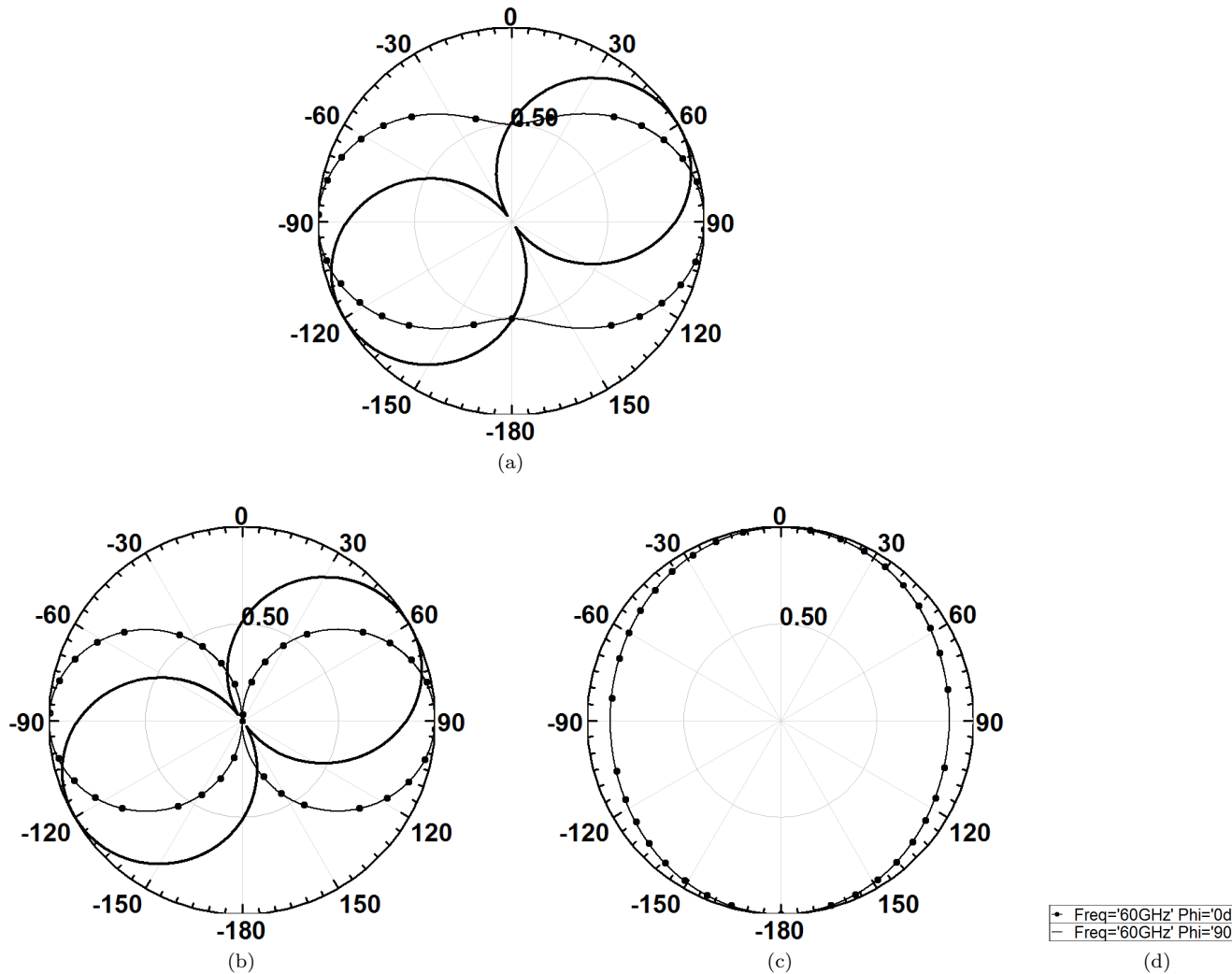
Figure 5.3: Radiation Pattern obtained by simulation in HFSS (a) E_T, (b) E_θ, (c) E_ϕ

5.2.4 Input and Radiation Resistance

The input impedance of an antenna is defined as the impedance offered by antenna at its input terminals. Input impedance is a complex quantity. Real part of input impedance is the input resistance. Radiation resistance is same as input resistance for lossless antenna and is related to total radiated real power.

Parameter	Value
Frequency(f)	60 GHz
Wavelength (λ)	5 mm
Arc Radius (a)	$\frac{\lambda}{4\pi} \approx 0.39$ mm
Length of dipole (l)	0.475λ

Table 5.1: Parameter list used while simulating in HFSS

Radiation resistance is found by using equation

$$P_{rad} = \frac{1}{2}|I_0|^2 R_{rad}$$

$$(5.48)$$

$$R_{rad} = \frac{2P_{rad}}{|I_0|^2}$$

Considering $\eta \approx 120\pi$, the value of radiation resistance is calculated approximately.

$$R_{in} = R_{rad} \approx 42\,\Omega \qquad\qquad (5.49)$$

5.3   Simulation Results

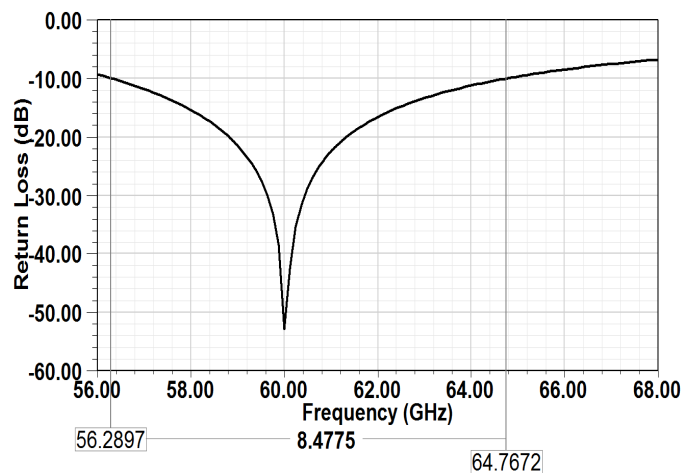
Figure 5.4: Return loss ($S11$) of proposed antenna.

In this section the obtained expressions for the antenna parameters are verified with the simulation results. For simulations HFSS tool is used. As thickness of the dipole increases, the bandwidth increases which reduces the resonating length of the dipole slightly. Also to make dipole resonant with no reactive component in antenna impedance, the length of dipole is reduced in practice.

Hence length of dipole is taken as 0.475λ instead of 0.5λ. Table 5.1 gives the parameters considered while simulating in HFSS.

The E fields given by equation 5.36, 5.37 and 5.38 plotted using MATLAB are shown in Figure 5.2. From the radiation pattern obtained using theoretical expression the dipole has maximum gain at elevation angle of 63° (approx.). Figure 5.3 shows radiation pattern of simulated antenna which has maximum at 61° (approx.) which is a good match with theoretically obtained value. The
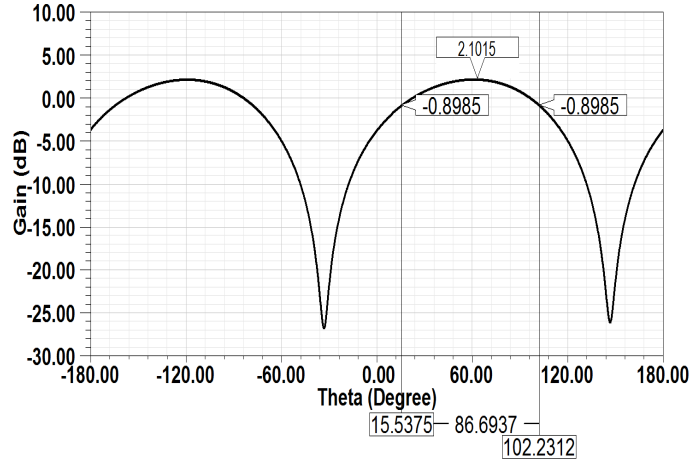
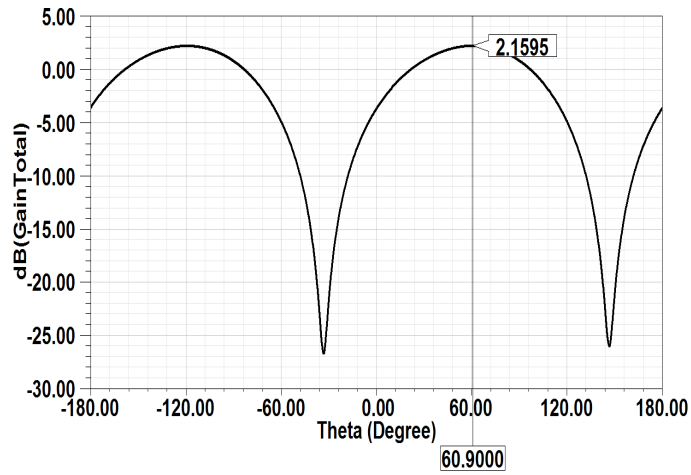Figure 5.5: 2D gain plot of proposed antenna.

Figure 5.6: 2D directivity plot of proposed antenna.

radiation pattern of antenna remains same in both plots obtained using MATLAB and HFSS.

Figure 5.3 to 5.7 shows plots for the simulated antenna using HFSS.

The return loss (S11 parameter) is shown in Figure 5.4 which shows that bandwidth of the antenna is 8GHz ranging from 56.28 GHz to 64.76 GHz which gives percentage bandwidth of 14%. From the gain plot depicted in Figure 5.5, it can be observed that Half Power Beam-width (HPBW) equals to 86.69° with a maximum gain of 2.10 dB at an elevation angle of 61° (approx.).

To verify the directivity found using theoretical analysis, directivity is plotted using HFSS. Theorotically directivity is 1.66 i.e. 2.20 dB at an elevation angle of 63°(approx.) whereas in simulation 2.15 dB directivity is obtained at an elevation angle of 61°(approx.) which is direction of maximum radiation.The 2D plot of directivity is given in Figure 5.6. Impedance at resonance shown in Figure 5.7 is 39 Ω approximately equal to theoretically obtained impedance.

From all the plots it is apparent that there exists a good match between theoretically obtained expressions for all the antenna parameters and simulated results.
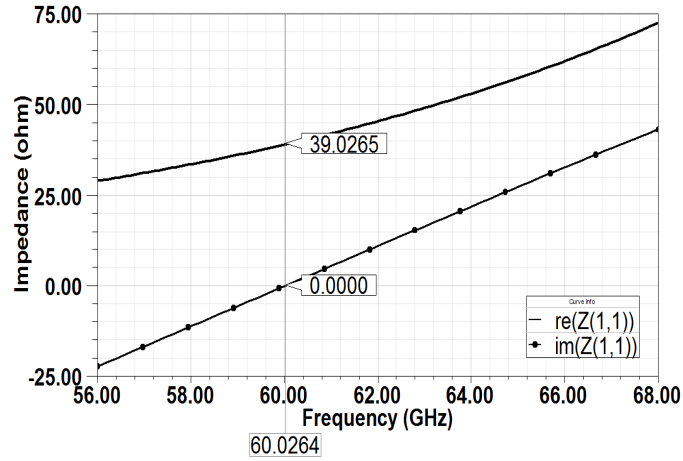
Figure 5.7: Impedance plot of proposed antenna.

5.4 Conclusion

A non-linear MM wave wire-dipole antenna has been designed for UWB applications. The effect of semi-circular curvature of the arms of dipole antenna on the performance has been investigated. The radiated fields and antenna parameters have been theoretically derived for proposed antenna. Theoretically obtained results have been validated by comparing with simulated antenna results using HFSS and satisfactory matching is observed. The non-linear geometry provides an ease in its fabrication, and can be embroidered on fabric.

Chapter 6

Conclusion and Future Work

6.1   Conclusion

This thesis comprises of antenna design along with the thorough study about MM wave antennas and its applications. To summarize, for the usage in unlicensed UWB band, four different configurations of antennas are designed and are validated through theoretical analysis and simulations. The major significance of these antenna designs can be realized by the fact that, they utilize almost entire UWB and also the return loss incurred is noticeably reduced which escalates the overall antenna performance. The analyses performed state that, the impedance and radiation patterns are almost same in all the cases. However, among the designs done it is observed that the antenna design (Antenna Design 4) with a pair of inverted L-shaped slots performed better in terms of return loss, bandwidth and overall characteristics of antenna. In addition to the above work, two antenna designs among the four proposed antennas are optimized and exhaustive analysis on the effect of the notches on the radiation patch has been carefully carried out, which resulted in optimal enhancement of bandwidth, radiation pattern and VSWR by simultaneous reduction in return losses. Hence it is surmised that these two optimized antennas give better results. However both the antennas exhibit similar radiation pattern. Noteworthy features of these optimized antennas are compact size, ability to work in UWB range with reduced return losses and enhanced performance due to minimal reflected power from the antenna.

Moreover, a non-linear geometry of antenna which comprises of two semi-circular arms of total half wavelength long is designed and antenna parameters have been derived theoretically. The effect of semi-circular curvature of the arms of dipole antenna on the performance has been investigated. The radiated fields and antenna parameters have been theoretically derived for proposed antenna. Theoretically obtained results have been validated by comparing with simulated antenna results.

The designed non-linear dipole antenna for MM wave applications utilizes whole available bandwidth of unlicensed UWB centered at 60 GHz. Radiation fields and derived results of antenna parameters are validated by comparing them with the simulation results. Simulation results show that this proposed geometry is radiating maximum at an elevation angle of $61°$. Directivity of the antenna is about 2.20 dB and input resistance is $42\,\Omega$. Half power beam width is $86.69°$. Operating bandwidth is around 8.5 GHz which ranges from 56.28 GHz to 64.76 GHz, hence it covers the un-licensed UWB at 60 GHz completely.

6.2 Future Work

Efficient Unlicensed UWB band antennas are designed in this work and proper analyses have been done for the proof of the proposed concepts. Future extension of this research work will be focused mainly on designing or exploring these antenna designs for body worn applications and BAN applications. In order to do so, effects of MM wave radiations on human body should be carefully analyzed. Moreover, effect on antenna performance in the close proximity of human body should also be exploited. Standards such as SAR which estimates the harmful effects and limits the antenna usage or application have to be considered while designing any antenna for BAN applications. In addition to these effects, the designed antenna for UWB body-centric communications must also be complaint to the requirements and constraints such as 1) optimized characteristics in both frequency and time domains; 2) compact size and low profile; 3) harmless and reliable on-body propagation. Owing to all these several constraints, designing a BAN antenna is indeed a challenging task, but considering the advantages and utilities that can be obtained from the same on the other hand, UWB BAN antenna design is one among the fascinating budding research topics.

References

[1] H. G. Schantz. Three centuries of UWB antenna development. In 2012 IEEE International Conference on UltraWideband. IEEE, 2012 506512.

[2] F. C. Commission et al. FCC Report and Order for Part 15 acceptance of ultra wideband (UWB) systems from 3.110.6 GHz. *FCC, Washington, DC* .

[3] P. Li, J. Liang, and X. Chen. Study of printed elliptical/circular slot antennas for ultrawideband applications. *IEEE Transactions on antennas and Propagation* 54, (2006) 16701675.

[4] J. Liang, C. C. Chiau, X. Chen, and C. G. Parini. Study of a printed circular disc monopole antenna for UWB systems. *IEEE Transactions on antennas and propagation* 53, (2005) 35003504.

[5] K. Ray and Y. Ranga. Ultrawideband printed elliptical monopole antennas. *IEEE transactions on antennas and propagation* 55, (2007) 11891192.

[6] C. A. Balanis. Antenna theory: analysis and design. John Wiley & Sons, 2016.

[7] M. Ammanii and Z. N. Chen. Wideband monopole antennas for multiband wireless systems. *IEEE Antennas and Propagation Magazine* 45.

[8] J. R. James and P. S. Hall. Handbook of microstrip antennas, volume 1. IET, 1989.

[9] J. Liang, C. C. Chiau, X. Chen, and C. G. Parini. Study of a printed circular disc monopole antenna for UWB systems. *IEEE Transactions on antennas and propagation* 53, (2005) 35003504.

[10] B. Ooi, G. Zhao, M. Leong, K. Chua, and C. L. Albert. Wideband LTCC CPWfed twolayered monopole antenna. *Electronics Letters* 41, (2005) 1.

[11] L. Lizzi, R. Azaro, G. Oliveri, and A. Massa. Printed UWB antenna operating over multiple mobile wireless standards. *IEEE Antennas Wireless Propag. Lett* 10, (2011) 14291432.

[12] J. Kim, T. Yoon, J. Kim, and J. Choi. Design of an ultra wideband printed monopole antenna using FDTD and genetic algorithm. *IEEE Microwave and Wireless Components Letters* 15, (2005) 395397.

[13] Z. Low, J. Cheong, and C. Law. Lowcost PCB antenna for UWB applications. *IEEE antennas and wireless propagation letters* 4, (2005) 237.

[14] O. Ahmed and A. Sebak. A printed monopole antenna with two steps and a circular slot for UWB applications. *IEEE Antennas and Wireless Propagation Letters* 7, (2008) 411413.

[15] C. Huang and W. Hsia. Planar elliptical antenna for ultrawideband communications. *Electronics Letters* 41, (2005) 296297.

[16] X. Zhang, W. Wu, Z. Yan, J. Jiang, and Y. Song. Design of CPWfed monopole UWB antenna with a novel notched ground. *Microwave and optical technology letters* 51, (2009) 8891.

[17] R. Azim, M. T. Islam, and N. Misran. Ground modified doublesided printed compact UWB antenna. *Electronics Letters* 47, (2011) 911.

[18] D. R. Melo, M. N. Kawakatsu, D. Nascimento, and V. Dmitriev. A planar monopole UWB antennas with rounded patch and ground plane possessing improved impedance matching. *Microwave and Optical Technology Letters* 54, (2012) 335338.

[19] X. Liang, S. Zhong, and W. Wang. Tapered CPWfed printed monopole antenna. *Microwave and optical technology letters* 48, (2006) 12421244.

[20] X. Liang, S. Zhong, W. Wang, and F. Yao. Printed annular monopole antenna for ultrawideband applications. *Electronics Letters* 42, (2006) 1.

[21] X. Liang, S. Zhong, and W. Wang. UWB printed circular monopole antenna. *Microwave and optical technology letters* 48, (2006) 15321534.

[22] S. Zhong, X. Liang, and W. Wang. Compact elliptical monopole antenna with impedance bandwidth in excess of 21: 1. *IEEE Transactions on Antennas and Propagation* 55, (2007) 30823085.

[23] J. Liu, S. Zhong, and K. P. Esselle. A printed elliptical monopole antenna with modified feeding structure for bandwidth enhancement. *IEEE Transactions on Antennas and Propagation* 59, (2011) 667670.

[24] I. Oppermann. M. Hama la inen and J. Iinatti UWB Theory and Applications, England 2004.

[25] N. Cravotta. Ultrawideband: the next wireless panacea? *EDNBOSTON THEN DENVER* 47, (2002) 5160.

[26] R. Ramasamyraja, M. Pandiguru, and V. Arun. Design of ultra wide band antenna for tactical communication in electronic warfare. In Communications and Signal Processing (ICCSP), 2014 International Conference on. IEEE, 2014 12561259.

[27] E. M. Staderini. UWB radars in medicine. *IEEE Aerospace and Electronic Systems Magazine* 17, (2002) 1318.

[28] I. Gresham, A. Jenkins, R. Egri, C. Eswarappa, N. Kinayman, N. Jain, R. Anderson, F. Kolak, R. Wohlert, S. P. Bawell et al. Ultrawideband radar sensors for shortrange vehicular applications. *IEEE Transactions on Microwave Theory and Techniques* 52, (2004) 21052122.

[29] K. Siwiak. UltraWideband Radio. Wiley Online Library, 2004.

[30] L. Yang and G. B. Giannakis. Ultrawideband communications: an idea whose time has come. *IEEE signal processing magazine* 21, (2004) 2654.

[31] Y. Tanabe, T. Uwano, and T. Baba. Design of E and H plane omnidirectional UWB half slot antennas. In Microwave Conference, 2009. APMC 2009. Asia Pacific. 2009 774–777.

[32] V. Kumar and B. Gupta. Swastika slot UWB antenna for body-worn application in WBAN. In Medical Information and Communication Technology (ISMICT), 2014 8th International Symposium on. 2014 1–5.

[33] J. Wu, Z. Zhao, M. Ellis, Z. Nie, and Q. H. Liu. Enhanced directivity and bandwidth of a stepped open-slot antenna with L-shaped slots and parasitic strip. *Microwaves, Antennas Propagation, IET* 8, (2014) 465–473.

[34] S. D. Raju, B. Haranath, and L. Panwar. Novel UWB Swastika slot antenna with concentric circular slots and modified ground plane with inverted L-shaped slots. In Advances in Computing, Communications and Informatics (ICACCI), 2015 International Conference on. IEEE, 2015 76–81.

[35] H. Iwasaki. A circularly polarized small-size microstrip antenna with a cross slot. *IEEE transactions on antennas and propagation* 44, (1996) 1399–1401.

[36] C.-Y. Huang, J.-Y. Wu, and K.-L. Wong. Cross-slot-coupled microstrip antenna and dielectric resonator antenna for circular polarization. *IEEE Transactions on Antennas and Propagation* 47, (1999) 605–609.

[37] Z. Pi and F. Khan. An introduction to millimeter-wave mobile broadband systems. *IEEE Communications Magazine* 49, (2011) 101–107.

[38] T. S. Rappaport, J. N. Murdock, and F. Gutierrez. State of the art in 60-GHz integrated circuits and systems for wireless communications. *Proceedings of the IEEE* 99, (2011) 1390–1436.

[39] T. S. Rappaport, S. Sun, R. Mayzus, H. Zhao, Y. Azar, K. Wang, G. N. Wong, J. K. Schulz, M. Samimi, and F. Gutierrez. Millimeter wave mobile communications for 5G cellular: It will work! *IEEE access* 1, (2013) 335–349.

[40] Z. Pi and F. Khan. An introduction to millimeter-wave mobile broadband systems. *IEEE Communications Magazine* 49, (2011) 101–107.

[41] T. S. Rappaport, J. N. Murdock, and F. Gutierrez. State of the art in 60-GHz integrated circuits and systems for wireless communications. *Proceedings of the IEEE* 99, (2011) 1390–1436.

[42] T. S. Rappaport, S. Sun, R. Mayzus, H. Zhao, Y. Azar, K. Wang, G. N. Wong, J. K. Schulz, M. Samimi, and F. Gutierrez. Millimeter wave mobile communications for 5G cellular: It will work! *IEEE access* 1, (2013) 335–349.

[43] o. N.-I. R. H. IEEE Standards Coordinating Committee 28. IEEE Standard for Safety Levels with Respect to Human Exposure to Radio Frequency Electromagnetic Fields, 3kHz to 300 GHz. Institute of Electrical and Electonics Engineers, Incorporated, 1992.

[44] o. N.-I. R. H. IEEE Standards Coordinating Committee 28. IEEE Standard for Safety Levels with Respect to Human Exposure to Radio Frequency Electromagnetic Fields, 3kHz to 300 GHz. Institute of Electrical and Electonics Engineers, Incorporated, 1992.

[45] M. Kojima, M. Hanazawa, Y. Yamashiro, H. Sasaki, S. Watanabe, M. Taki, Y. Suzuki, A. Hirata, Y. Kamimura, and K. Sasaki. Acute ocular injuries caused by 60-GHz millimeter-wave exposure. *Health physics* 97, (2009) 212–218.

[46] H. A. Kues, S. A. D'Anna, R. Osiander, W. R. Green, and J. C. Monahan. Absence of ocular effects after either single or repeated exposure to 10 mW/cm2 from a 60 GHz CW source. *Bioelectromagnetics* 20, (1999) 463–473.

[47] F. A. Duck. Physical properties of tissues: a comprehensive reference book. Academic press, 2013.

[48] O. P. Gandhi and A. Riazi. Absorption of millimeter waves by human beings and its biological implications. *IEEE Transactions on Microwave Theory and Techniques* 34, (1986) 228–235.

[49] C. Alabaster. Permittivity of human skin in millimetre wave band. *Electron. Lett* 39, (2003) 1521–1522.

[50] S. Gabriel, R. Lau, and C. Gabriel. The dielectric properties of biological tissues: III. Parametric models for the dielectric spectrum of tissues. *Physics in medicine and biology* 41, (1996) 2271.

[51] S. Alekseev and M. Ziskin. Human skin permittivity determined by millimeter wave reflection measurements. *Bioelectromagnetics* 28, (2007) 331–339.

[52] C. Pozrikidis. Numerical computation in science and engineering, volume 6. Oxford university press New York, 1998.